automation

MDPI

Article

Design and Modeling of an Intelligent Robotic Gripper Using a Cam Mechanism with Position and Force Control Using an Adaptive Neuro-Fuzzy Computing Technique

Imad A. Kheioon [1], Raheem Al-Sabur [1,*] and Abdel-Nasser Sharkawy [2,3,*]

[1] Mechanical Department, Engineering College, University of Basrah, Basrah 61004, Iraq; imad.kheioon@uobasrah.edu.iq
[2] Mechanical Engineering Department, Faculty of Engineering, South Valley University, Qena 83523, Egypt
[3] Mechanical Engineering Department, College of Engineering, Fahad Bin Sultan University, Tabuk 47721, Saudi Arabia
* Correspondence: raheem.musawel@uobasrah.edu.iq (R.A.-S.); abdelnassersharkawy@eng.svu.edu.eg or eng.abdelnassersharkawy@gmail.com (A.-N.S.)

Abstract: Manufacturers increasingly turn to robotic gripper designs to improve the efficiency of gripping and moving objects and provide greater flexibility to these objects. Neuro-fuzzy techniques are the most widespread in developing gripper designs. In this study, the traditional gripper design is modified by adding a suitable cam that makes it compatible with the basic design, and an adaptive neuro-fuzzy inference system (ANFIS) is used in a MATLAB Simulink environment. The developed gripper investigates the follower path concerning the cam surface curve, and the gripper position is controlled using the developed ANFIS-PID. Three methods are examined in the developed ANFIS-PID controller: grid partitioning (genfis1), subtractive clustering (genfis2), and fuzzy C-means clustering (genfis3). The results show that the added cam can improve the gripping strength and that the ANFIS-PID model effectively handles the rise time and supported settling time. The developed ANFIS-PID controller demonstrates more efficient performance than Fuzzy-PID and traditional tuned-PID controllers. This proposed controller does not achieve any overshoot, and the rise time is improved by approximately 50–51%, and the steady-state error is improved by 75–95%, compared with Fuzzy-PID and tuned PID controllers. Moreover, the developed ANFIS-PID controller provides more stability for a wide range of set point displacements—0.05 cm, 0.5 cm, and 1.5 cm—during the testing period. The developed ANFIS-PID controller is not affected by disturbance, making it well suited for robotic gripper designs. Grip force control is also investigated using the proposed ANFIS-PID controller and compared with the Fuzzy-PID in three scenarios. The result from this force control proves objects' higher actual gripping performance by using the proposed ANFIS-PID.

Keywords: robotic gripper design; cam mechanism; intelligent ANFIS-PID technique; position and force control; modeling and comparison

Academic Editor: Felipe Martins

Received: 1 December 2024
Revised: 13 January 2025
Accepted: 17 January 2025
Published: 18 January 2025

Citation: Kheioon, I.A.; Al-Sabur, R.; Sharkawy, A.-N. Design and Modeling of an Intelligent Robotic Gripper Using a Cam Mechanism with Position and Force Control Using an Adaptive Neuro-Fuzzy Computing Technique. *Automation* **2025**, *6*, 4. https://doi.org/10.3390/automation6010004

1. Introduction

Intelligent robotic grippers have significantly contributed to technological advancements over the past decade, as their use has grown steadily in various industries [1]. Industrial automation is the broadest area of use for robotic grippers, where the main targets are picking up, holding, and manipulating objects [2,3]. Complex operation activities requiring high precision and dexterity in the assembly process still require new tools

and methods to deliver excellent performance [4,5]. As a result, much research is being conducted on designing robot grippers to increase industrial precision and dexterity.

There are no specific classifications for the types of robotic grippers; they can be classified based on their working principles, modes of action, or key parameters. The classification based on the working principle is the most popular in industrial robotic grippers. Figure 1 provides an explanation to highlight the types in this classification. The most used types are mechanical grippers, also known as fingered grippers, which typically consist of two or more fingers, depending on the specific application [6,7]. Vacuum gripper suction cups create a vacuum between the object's surface and the gripper, enabling the gripper to pick up objects [8,9]. Magnetic grippers employ a magnetic field to elevate ferromagnetic materials like steel [10]. When lifting thin materials becomes necessary, robotic grippers, made of flexible and soft materials, often operate in parallel with other types, most notably pneumatic grippers. Adhesive grippers serve smooth, thin, and soft surfaces that do not require significant lifting force [11]. When the classification is based on actuation methods, the most popular types are pneumatic grippers, electric grippers, hydraulic grippers, and servo-electric grippers, and each type has its advantages and limitations depending on the use case [12]. When the classification is based on key parameters in robotic grippers, many types emerge, such as grip force, stroke length, payload capacity, grip precision, and feedback [13].

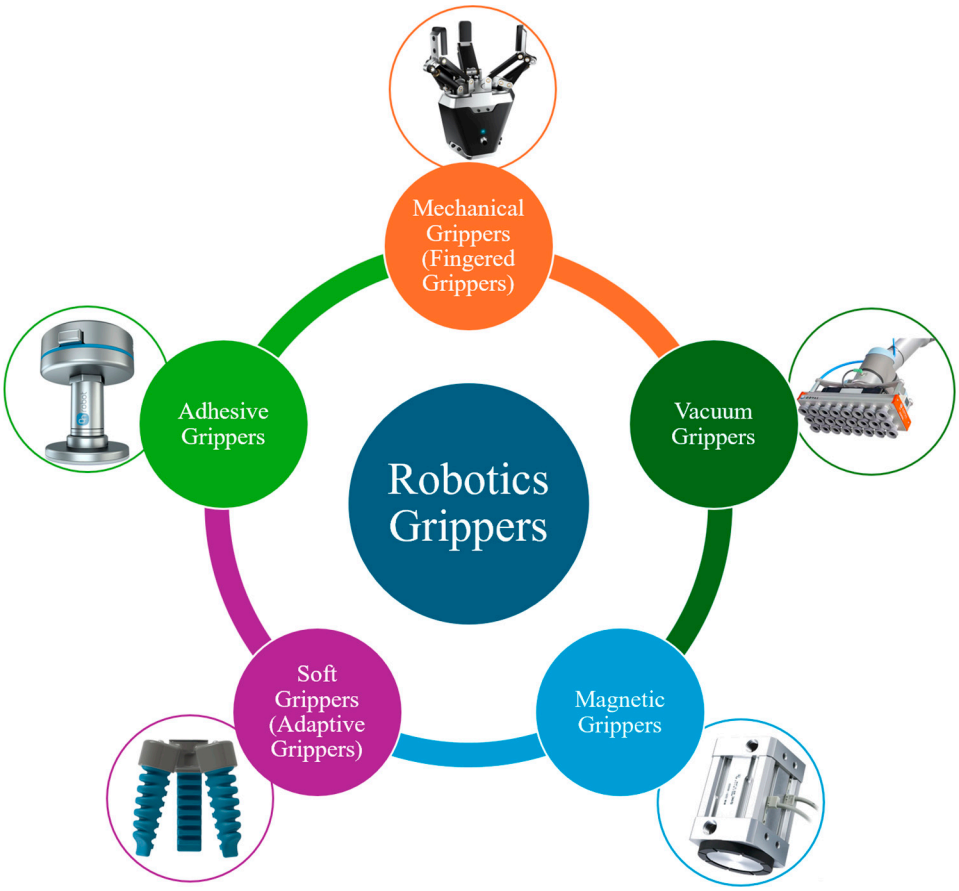

Figure 1. Main robotic grippers classified by working principle.

Well-established methods for controlling robots in structured environments rely on synthesizing and analyzing mathematical modeling accuracy [14]. Sensor inaccuracy creates complex issues for predicting objects' attributes in unstructured environments. Fuzzy-controlled techniques are quite common in the design of robotic grippers. These

grippers are based on basic parameters that are often related to weight, shape, and the friction required between them and the objects to be moved [15]. In studies of grippers controlled by fuzzy techniques, Vaishnav and Khan [16] and Tamilselvan and Aarthy [17] emphasized that minimizing errors and derivatives are the most crucial factors to consider. It should be noted that PI and PD controllers do not perform optimally in reducing transient response and steady-state response errors, respectively. Therefore, the PID controller is considered the most widely used. Despite its acceptability, the system performance in the PID controller can be affected and accompanied by instability in many cases, especially when nonlinearities are introduced into the system dynamics [18,19]. Yager and Zadeh [20] and Somwanshi et al. [21] showed that the drawbacks of classical linear PID controllers can be avoided or have their effects reduced by fuzzy controllers because it has enough flexibility to deal with nonlinear cases. Aslinezhad et al. [22] developed a pneumatic finger-like actuator for medical purposes based on an adaptive neuro-fuzzy inference system and showed that Gaussian, trapezoidal, and triangular shapes are necessary for optimizing fuzzy controller operations. Nguyen et al. [23] designed a compliant gripper mechanism using a hybrid system of an ANFIS and fuzzy logic, considering frequency values and displacement values as response parameters, and simulating the proposed model with a finite element. The flexure gripper was the focus of a study by Dinhet et al. [24], where they created an optimization framework by combining an ANFIS and the Taguchi optimization method. Their findings demonstrated the ability to reduce the standard deviation to zero, and the developed model outperformed other techniques, particularly for the flexure gripper. Huynh and Kuo [25] used gradient descent iterative learning control to find the best design for a robot gripper based on fuzzy rule-based design while holding unknown objects and going through an iterative learning control process. Mukhtar et al. [26] showed that using a multi-system ANFIS can make it more efficient as one fuzzy controller can replace four systems in controlling an ambidextrous robot arm, and they showed that the developed model was more efficient, stable, and less energy-consuming. Bahedh et al. [27] developed a model to increase the efficiency of a robotic gripper by adding a cam to a Fuzzy-PID controller using MATLAB Simulink. They demonstrated that the developed gripper produced encouraging results by tracking the paths in the cam surface curve where it exceeded the maximum percentage and that it achieved ideal results for each rising time, settling time, and steady-state error. Hazem and Bingül [28] proposed a radial-basis neuro-fuzzy LQR-based controller for achieving a desired torque for an inverted pendulum. Their method improved the stability of the system and its robustness against external disturbances.

The literature mentioned above suggests that robotic gripper design is still of great interest, with multiple directions for its development and the possibility of combining more than one approach. Controlling the position and force of the gripper needs further investigation and evaluation using intelligent methods and techniques.

This paper's main contribution and novelty lies in confronting an important configuration gap for improving robotic gripper design. The main contribution is presented in the following points:

- The proposed gripper design was developed by adding a suitable cam that makes it compatible with the basic design. In addition, the cam is used to improve the strength of the gripper.
- An intelligent adaptive neuro-fuzzy inference system (ANFIS) was used for this gripper design.
- The main objective of this proposed gripper design was to investigate the follower path of the cam surface curve and to improve motion performance.

- The ANFIS-PID system considers the position control of the gripper to achieve accurate positioning, which is necessary to keep the object safe.
- For this purpose, three methods were examined in the developed ANFIS-PID controller, which are grid partitioning (genfis1), subtractive clustering (genfis2), and fuzzy C-means clustering (genfis3).
- MATLAB Simulink was used to apply the ANFIS system to the gripper design.
- A comparison is executed between the results of the proposed ANFIS-PID and other controllers, such as traditional PID and Fuzzy-PID.
- Different scenarios were applied to the proposed controller to investigate its effectiveness, such as the use of different displacements of the robotic gripper and the effect of the disturbances.
- Grip force control was conducted and investigated with the proposed ANFIS to evaluate the actual gripping performance of objects. In this case, the performance of the proposed ANFIS-PID is compared with Fuzzy-PID. Three different scenarios were investigated to present the efficiency of the proposed controller. All these simulations were implemented in MATLAB.

The outline of the rest of this paper is presented as follows: Section 2 shows the materials and methods. This section discusses the ANFIS technique and the gripper design. In addition, the performed simulation modeling, including the inputs and outputs of the ANFIS, is presented for both position and force control applications. Section 3 presents the results of the gripper position control. The proposed controller is investigated using different scenarios, and the current results are compared with traditional PID and Fuzzy-PID results. Section 4 presents the grip force control using the proposed ANFIS-PID and compares it with Fuzzy-PID. Finally, Section 5 concludes this paper, offering remarks on the proposed controller, commenting on its limitations, and suggesting future work on it.

2. Materials and Methods

This section discusses the proposed neuro-fuzzy computing technique, the proposed design of the robotic gripper using a cam mechanism, and the Simulink modeling, for both position and force control applications. All these are discussed in the following subsections.

2.1. Neuro-Fuzzy Technique

Control systems have been steadily developing for the last decade, and it has become clear that hybrid control systems can be more effective than traditional systems. Hybrid control systems are characterized by their relevance to real-world problems because they combine different techniques, such as neural networks and genetic algorithms, in addition to fuzzy logic and rely directly on expert systems [29]. Thus, they begin to behave in a way that is remarkably like the human mind when dealing with cognitive uncertainties. This integrated system can be described as being neuro-fuzzy. Models built on these systems are characterized by two scenarios: linguistic statements and multiple layers [30]. In the first scenario, the fuzzy interface block acts as an input to a neural network, often multi-layered, that can be adapted (by training) later to give the required decisions (outputs), as shown in Figure 2a. In the second scenario, a multi-layered neural network drives the fuzzy inference mechanism, as shown in Figure 2b. Neural networks' main function in neuro-fuzzy techniques is to tune membership functions in systems, which can appear in different forms, such as those in Figure 2c.

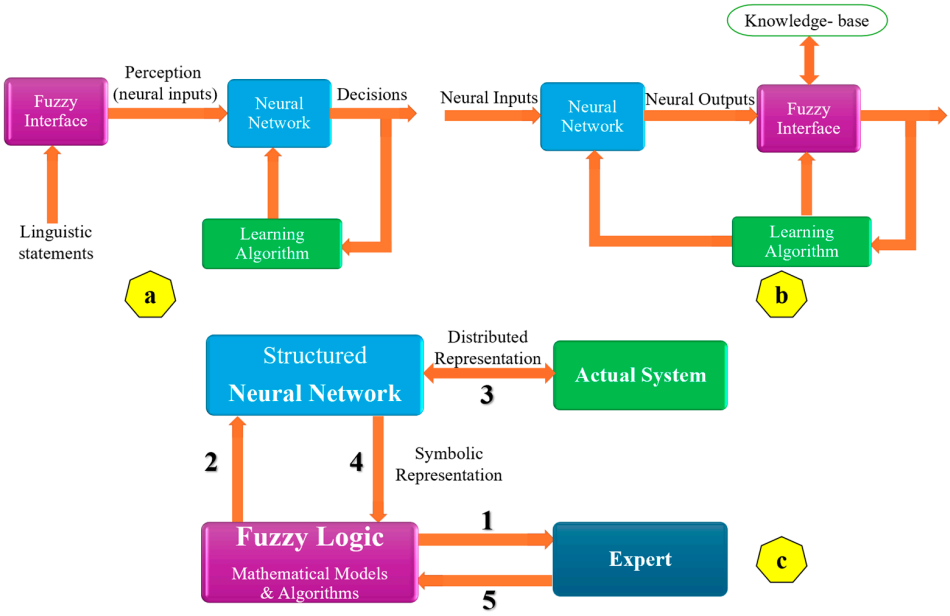

Figure 2. Structures of several fuzzy neural systems. (**a**) The fuzzy interface block acts as an input to a neural network, (**b**) A neural network drives the fuzzy inference mechanism, and (**c**) Neural network's function in neuro-fuzzy techniques to tune membership functions in system.

Jang laid the foundations for the adaptive network-based fuzzy inference system (ANFIS) in the early 1990s [31], and the TSK trio team (Takagi, Sugeno, and Kang) later developed it [32], as shown in Figure 3. The ANFIS system has many advantages that motivated us to use it, such as its ability to execute the learning process faster as well as its ability to model and estimate complex patterns and nonlinear systems efficiently and correctly. It has many applications across different fields, achieving high performance, as presented in [33–35]. An ANFIS typically consists of five layers or sequential stages, starting with the fuzzy layer (input membership functions), rule layer, normalization layer, and consequent (defuzzification) layer and concluding with the output layer [36]. In the ANFIS environment, nodes can be square, indicating the TSK fuzzy system's membership functions, or circular, non-modifiable, and static, dedicated to specifying maximum and minimum limits as well as multiplication operations. The improvements introduced by Sugeno have made the system more computationally efficient and ideal for mathematical analysis [37]. It has also become flexible in dealing with linear techniques such as PID, making it suitable for optimization and adaptive techniques [38,39].

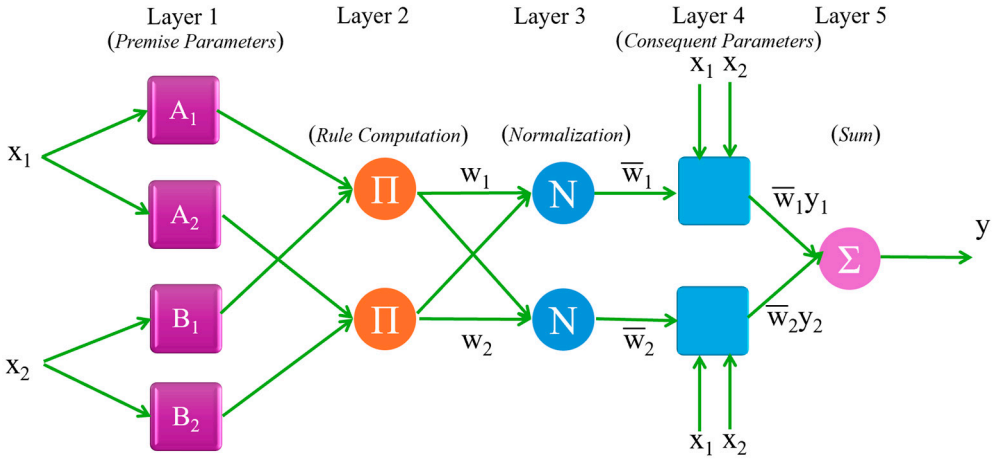

Figure 3. Adaptive network-based fuzzy inference system (ANFIS).

The rules and firing levels laid down by Sugeno and Takagi form the rationale for the ANFIS as indicated below [40]:

$$\left.\begin{array}{l} R_1 : \text{if x is } A_1 \text{ and y is } B_1 \text{ then } z_1 = a_1x + b_1y \\ R_2 : \text{if x is } A_2 \text{ and y is } B_2 \text{ then } z_2 = a_2x + b_2y \end{array}\right] \quad (1)$$

$$\left.\begin{array}{l} \alpha_1 = A_1(x_o) \times B_1(y_o) \\ \alpha_2 = A_2(x_o) \times B_2(y_o) \end{array}\right] \quad (2)$$

The equations below can describe the relationships that govern the outputs of individual rules and crisp control actions, where β_1 and β_2 are the normalized values of α_1 and α_2 with respect to the sum (α_1 + α_2):

$$\left.\begin{array}{l} z_1 = a_1(x_o) \times b_1(y_o) \\ z_2 = a_2(x_o) \times b_2(y_o) \end{array}\right] \quad (3)$$

$$\left.\begin{array}{c} z_o = \frac{\alpha_1 z_1 + \alpha_2 z_2}{\alpha_1 + \alpha_2} = \beta_1 z_1 + \beta_2 z_2 \\ \beta_1 = \frac{\alpha_1}{\alpha_1 + \alpha_2} \\ \beta_2 = \frac{\alpha_2}{\alpha_1 + \alpha_2} \end{array}\right] \quad (4)$$

Usually, in the first layer, bell-shaped membership functions represent the linguistic terms according to the parameter set $\{a_{i1}, a_{i2}, b_{i1}, \text{ and } b_{i2}\}$, as shown below:

$$\left.\begin{array}{l} A_i(u) = \exp\left[-\frac{1}{2}\left(\frac{u-a_{i1}}{b_{i1}}\right)^2\right] \\ B_i(v) = \exp\left[-\frac{1}{2}\left(\frac{u-a_{i2}}{b_{i2}}\right)^2\right] \end{array}\right] \quad (5)$$

In gripper position control, the inputs of the proposed ANFIS are as follows: x_1 is the position error, and x_2 is the derivative of the position error. In the gripper force control, the inputs of the proposed ANFIS are as follows: x_1 is the error in the controlled force, and x_2 is the derivative of the force error. The output y of the ANFIS is one gain of the PID controller (Kp, Ki, or Kd), where Kp is the proportional gain, Ki is the integral gain, and Kd is the derivative gain.

2.2. The Proposed Gripper Design

The construction of the gripper system and governing equations have been described in detail in [27], some of which will be referred to in this study.

Cam and gear mechanisms are very effective tools in motion transmission and are widely used in the design of robotic grippers. Grippers based on cam mechanisms have been used before in previous research papers, and their results were outstanding and effective. The research using cam mechanisms in gripper design can be found in [41–43]. The proposed gripper is designed based on an electromechanical system: a cam mechanism driven by an electric motor. Furthermore, to avoid complexity, a simple cam mechanism has been designed. Figure 4a indicates the main construction of the system, including the spring arrangement mechanism and the added cam, while Figure 4b indicates the proposed dimensions of the added cam.

In this model, an armature-controlled DC motor produces the necessary motor torque, as depicted in Figure 5a, and directs it towards the cam, enabling object grasping, as illustrated in Figure 5b. The equations of the proposed system are presented in the following points.

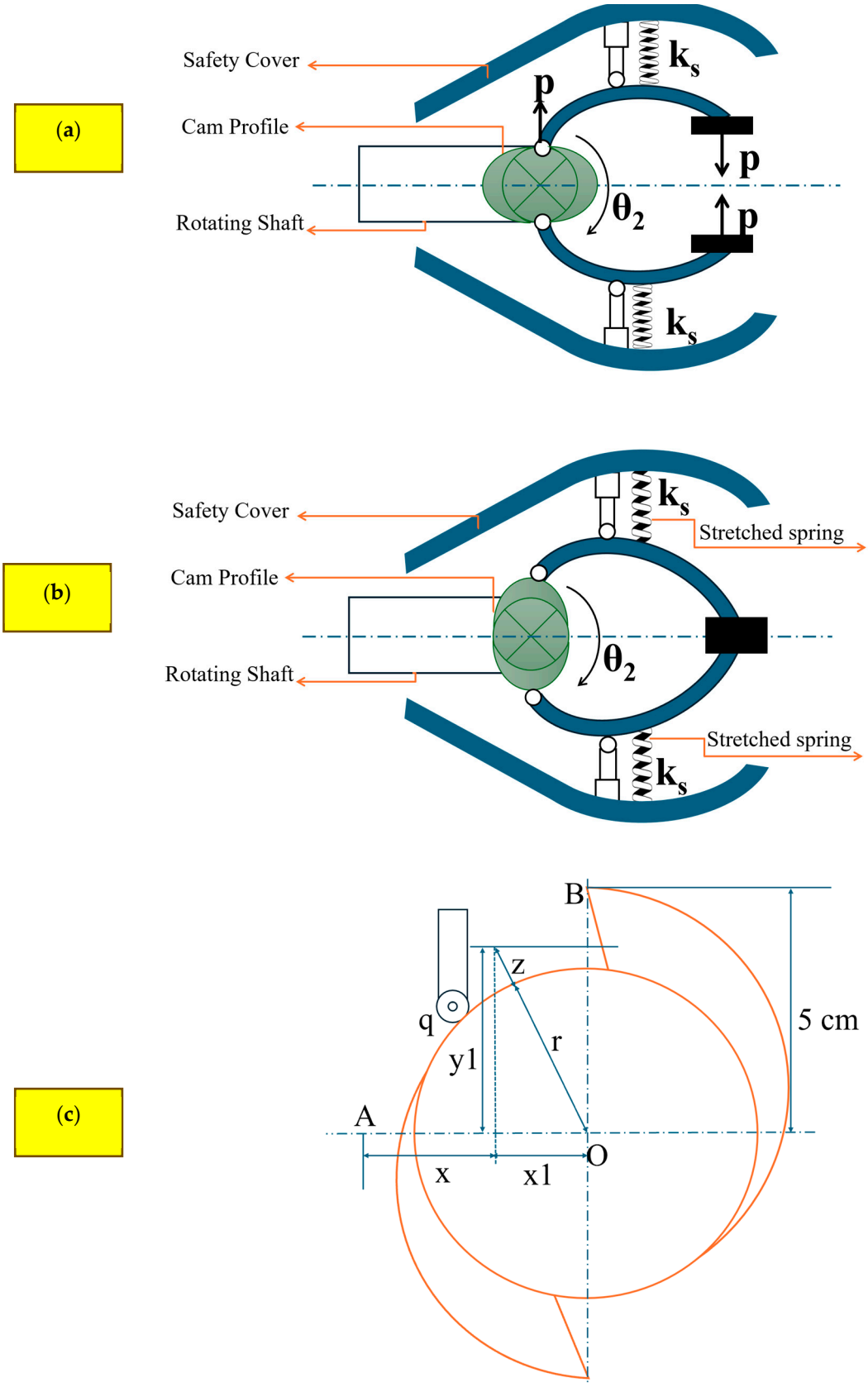

Figure 4. The main construction of the system. (**a**) The open case of the proposed gripper, (**b**) the closed case of the proposed gripper, and (**c**) the cam profile.

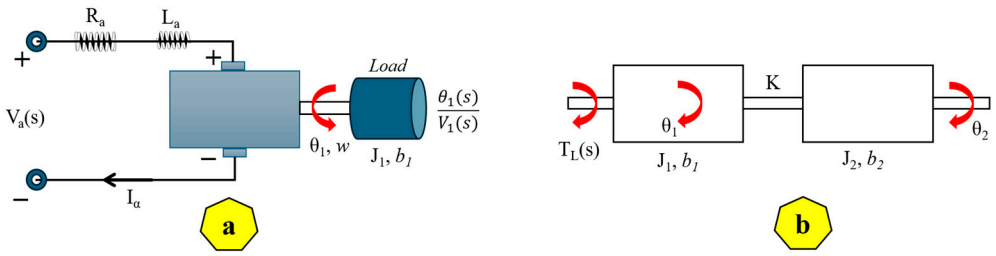

Figure 5. Schematic of the (**a**) DC motor loading and (**b**) torque effect on the DC motor. w represents the angular speed of the motor.

The torque produced by the DC motor (T_m) can be written as follows:

$$T_m(s) = K_m \, I_a(s) \tag{6}$$

where K_m represents the permeability function of magnetic material and I_a is the armature current. This current can be calculated with respect to input voltage V_a as follows:

$$V_a(s) = (R_a + L_a s) I_a(s) + V_b(s) \tag{7}$$

where R_a is armature resistance, L_a is armature inductance, and V_b is feedback voltage that comes from the sensor. From Equations (6) and (7), the torque of motor can be rearranged as follows:

$$T_m = \left(\frac{V_a(s) - V_b(s)}{R_a + L_a s} \right) \times K_m \tag{8}$$

The net load torque can be derived as follows:

$$T_L(s) = T_m(s) - T_d(s) \tag{9}$$

The equations of motion for the rotating part of the motor and gripper can be written in Laplace form as follows:

$$T_L = J_1 s^2 \, \theta_1(s) + b_1 s \theta_1(s) + K(\theta_1(s) - \theta_2(s)) \tag{10}$$

$$J_2 s^2 \, \theta_2(s) + b_2 s \theta_2(s) = K(\theta_1(s) - \theta_2(s)) \tag{11}$$

where b_1 is the damping coefficient of the DC motor parts, b_2 is the damping coefficient of the cam assembly, J_1 is the moment of inertia of the rotating part of the DC motor, J_2 is the moment of inertia of the rotating part of the cam assembly, K is the stiffness constant of the shaft, and θ_1 and θ_2 are positions of the angle input and output, respectively.

Equation (11) can be rearranged to be as follows:

$$k\theta_1(s) = \left(J_2 s^2 + b_2 s + k \right) \theta_2(s) \tag{12}$$

For the gripper mechanism, the following equations can be formulated as follows:

$$y_1 = (r + z) \sin(\theta_2) \tag{13}$$

$$(r + z) \cos(\theta_2) + x = 5 \tag{14}$$

From the properties of triangle similarity, it can be concluded that ($y_1 = x$), which leads to

$$(r + z) \, (\sin(\theta_2) + \cos(\theta_2)) = 5 \tag{15}$$

where z is the distance from the circumference of the base circle to the cam profile and r is the radius of the base circle of the cam in cm.

Then, z can be determined as follows [27]:

$$z = \frac{5}{\sin(\theta_2) + \cos(\theta_2)} - r \tag{16}$$

Then, knowing that $r = 5 \sin 45$ and $p = z \sin 45$, the vertical of each part of the gripper can be calculated as follows [27]:

$$p = \left(\frac{5}{\sin(\theta_2) + \cos(\theta_2)} - 5 \sin(45) \right) \sin(45) \tag{17}$$

where p is the position of the gripper or the linear displacement from the cam pushing the gripper in the direction of the sample or the object.

For the PID controller, the general form of transfer function can be written as follows:

$$\frac{U(s)}{E(s)} = Kp + \frac{KI}{s} + Kds \tag{18}$$

where Kp is the proportional gain, which is estimated by an ANFIS of the $genfis1$ type, KI is the integral gain, which is estimated by an ANFIS of the $genfis2$ type, and Kd is the derivative gain estimated by an ANFIS of the $genfis3$ type.

2.3. The Simulink Modeling

This study designed a self-adjusting intelligent controller based on the ANFIS method, using MATLAB Simulink to tune the three main parameters of the PID controller.

Many previous research works have been executed in a modeling and simulation environment, both in robotic and other fields. Therefore, we follow, in this paper, the same methodology by applying our proposed approach in the simulation environment (MATLAB), similarly to previous studies that have designed robotic grippers, such as [44–48]. These references are a few examples of the use of simulation environments, and there are many other such research works.

Many key parameters of the ANFIS are considered, such as the step size and its increasing and decreasing rates, the type and number of memberships of inputs, the method of dividing the data of inputs into appropriate sets, and learning algorithm parameters such as the learning rate and number of epochs. Also, the construction of a rule base plays a significant role in the efficiency of ANFIS behavior.

The typical inputs in the ANFIS model are the error in quantity and the rate in change in this error. However, in this study, the inputs are the error in position and control force and the rates of the change in these errors. While the output in the ANFIS model is any required variable or control signal that leads to control of the system for the desired behavior, in this study, the outputs of the ANFIS are the main three parameters of the PID controller. The antecedent is the event after the "if" statement, which represents the error in position or control force as well as their rates defined with number of memberships. The consequence is the event after the "then" statement, which represents, in this study, the proportional gain, integral gain, or derivative gain of the PID controller in order to implement the intelligent adaptive PID controller. The range of data is divided automatically with respect to the strategy of obtaining the membership of the inputs. It just needs to arrange the inputs in the columns, and the end column must be for the required output.

The Sugeno method has been widely used in previous research [49–51]. In the Sugeno method, the ANFIS method can deal with several inputs with a unique output; thus three of ANFIS methods ($genfis1,\ 2,$ and 3) were used to tune the PID factors [52], as shown in

Figure 6a. The inputs of the proposed ANFIS in developing the gripper position control were the position error and its derivative, where the output was one of the PID gains (Kp, Ki, or Kd). The inputs and outputs of the proposed ANFIS in developing the gripper force control are shown in Figure 6b. In position control, the ANFIS converts the error and its derivative into an appropriate range in the member according to the required rules until it reaches the preferred final output, as shown in Figure 7a. The Simulink model of the proposed ANFIS in developing the gripper force control is presented in Figure 7b.

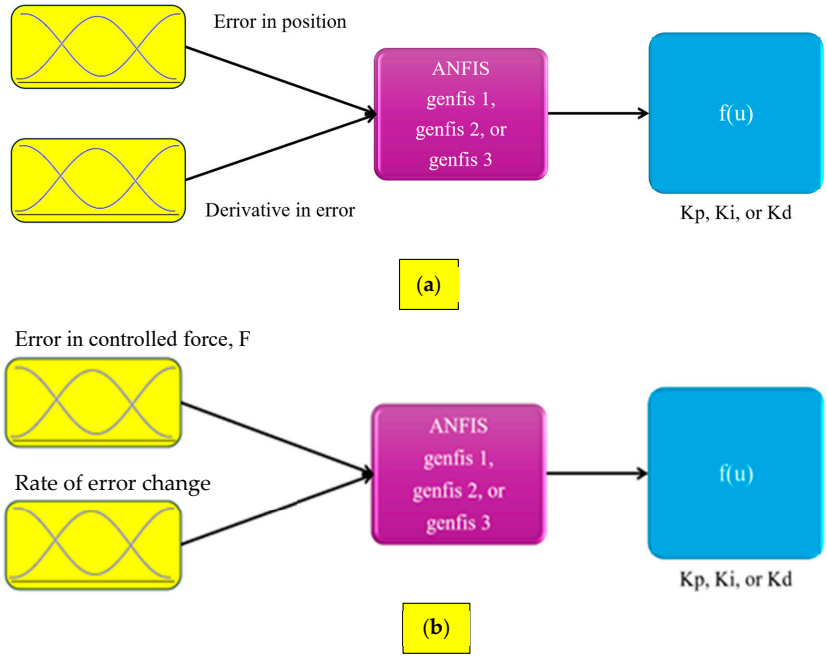

Figure 6. Inputs and output of ANFIS: (**a**) in gripper position control and (**b**) in gripper force control.

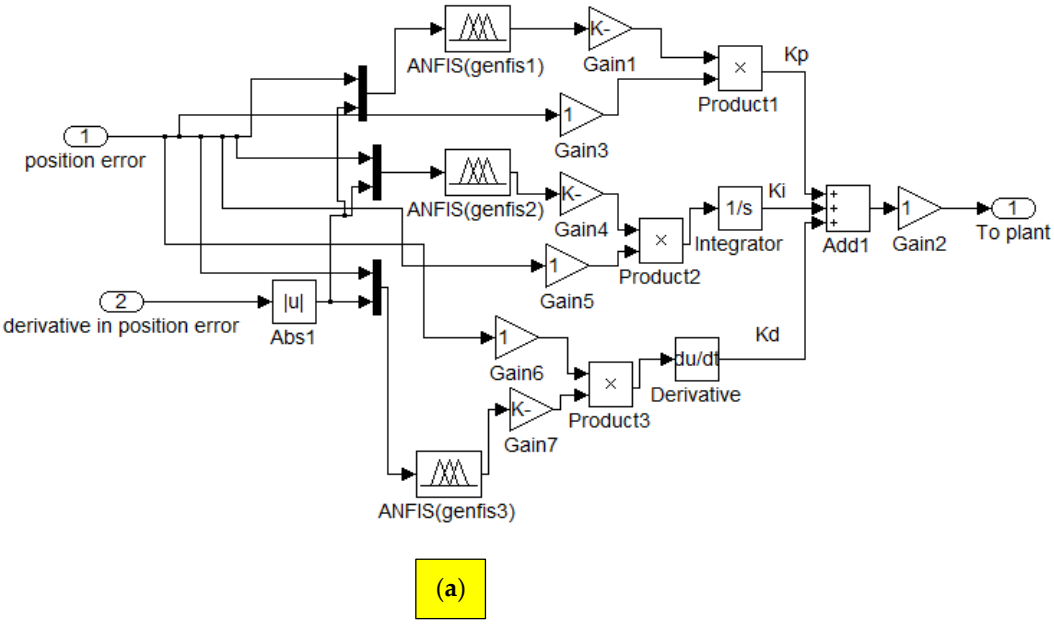

Figure 7. *Cont.*

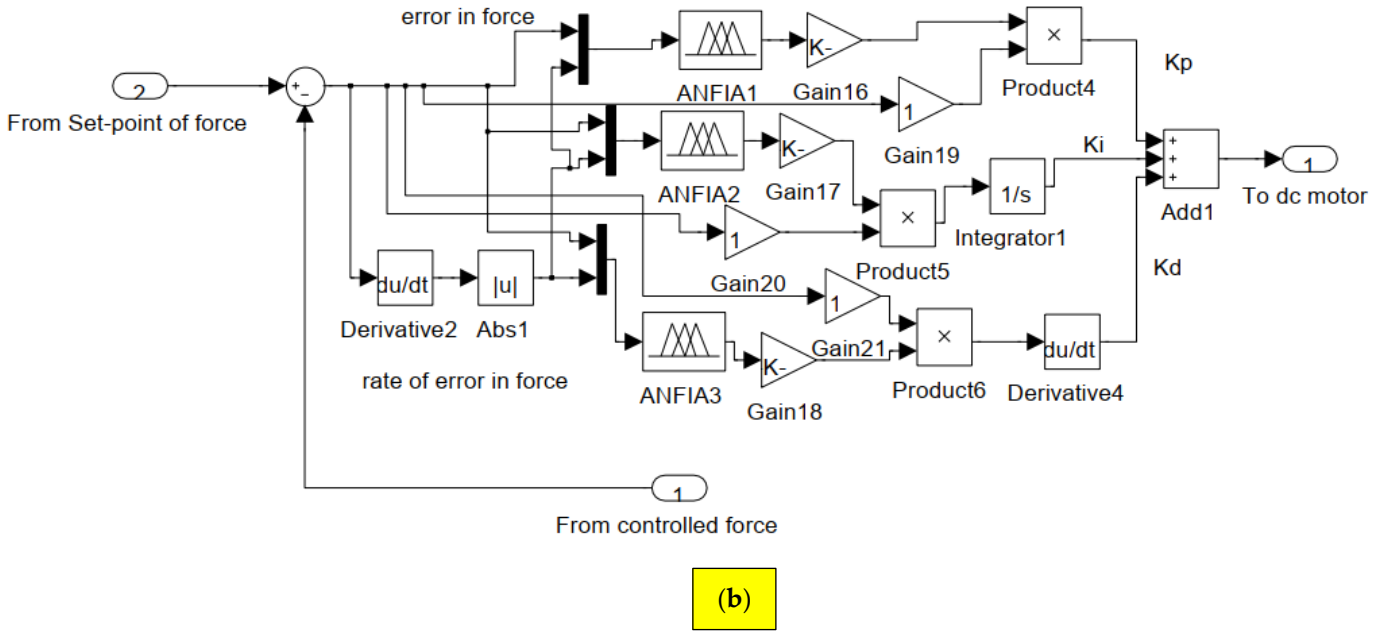

Figure 7. Simulink model of ANFIS-PID controller: (**a**) in developing the gripper position control and (**b**) in developing the gripper force control.

Many types of membership can be used for representing the inputs, such as the triangular membership function, trapezoidal membership function, Gaussian distribution curve, generalized bell membership function, and sigmoidal membership function. The type of the membership curve plays an important role in the operation of the controller, which depends on the ANFIS through its effect on the degree of membership inputs, which in turn affects the result of the conditions and thus will affect the controller's decision for the appropriate value for the outputs. However, after experimentation, the Gaussian distribution curve was used in this research to suit the data related to the type of application used.

3. Gripper Position Control: Results and Discussion

This section shows and discusses the results of the proposed ANFIS in controlling the position of the designed robotic gripper. The results are divided into two main sections: the first is the comparative analysis of FIS generation methods in the ANFIS: $genfis1$, 2, and 3. In contrast, the second is related to assessing the developed model at different displacements of the robotic gripper to find the best design and ideal control method.

The values of the main parameters used in the proposed simulation are presented in Table 1.

Table 1. The values of the main parameters used in the simulation of position control applications.

Parameter	Magnitude
r	3.5 cm
b_1	0.03 N·m·s
b_2	8 N·m·s
J_1	0.02 kg·m^2
J_2	0.05 kg·m^2
Motor constant, Km	0.023 N·m/A
Back electromotive gain, Kb	0.023 V/rad
La	0.23 Henry
Ra	1 Ω

There are certainly differences among the three methods of ANFIS in terms of the formation of the memberships and rules, which in turn affect the outputs of each method. The *genfis*1 method generates memberships by dividing the data equally and according to the required number to cover the entire range of the data. The number of rules is the product of the memberships for all inputs. The *genfis*2 method divides the data into groups according to a specific radius, and the number of rules is the number of memberships generated for each input, which are equal. As for the *genfis*3 method, the memberships are generated according to the required number and through an objective function; the method divides the data into the best groupings that suit the nature of the data, and the number of rules is the amount of data. This difference in the method of generating the rules and memberships has an impact on the speed of training as well as the flexibility in dealing with changes in inputs and the flexibility in determining appropriate output values. However, in the current research, the aim is not to study the differences between these methods because the *genfis*1 method is adopted for controlling and predicting the proportional part of the PID controller, the *genfis*2 method is adopted for controlling and predicting the integral part of the PID controller, and the *genfis*3 method is adopted for the purpose of controlling and predicting the derivative part of the PID controller, and the training data for the outputs are different for each method, so there is no opportunity to test the differences between these methods.

The rule base of the ANFIS method is formed automatically and according to each method (*genfis*1, 2, and 3). In the *genfis*1 method, the number of rules represents the number of the product of the memberships of the inputs so that each membership of the first input will produce one rule for each membership of the second input to ensure that all possibilities of changing the inputs are included. Therefore, in this work, there were 25 rules because each input has 5 memberships. In the *genfis*2 method, the data are divided according to a radius that represents the extent of the influence in each cluster, and the clusters are equal for the inputs and the output, which is the same number of the required rules, as in this work for this method there were three rules. In the *genfis*3 method, the number of clusters is determined by the user, and the method automatically guesses the estimated centers for the clusters and then determines an objective function that represents the shortest distance for the data from the centers, and the process is repeated until it reaches the best clusters to divide the data into, and the rules are the number of these clusters. The number and nature of the rule base play a clear role in the operation of the control system by making the appropriate decision for the value of the outputs that suit the nature and values of the inputs to the system.

The main learning parameters are the learning algorithm, such as a combination of backpropagation and least squares or backpropagation alone. Also, the number of epochs and the error goal are very important for adjusting the stooping criteria and reaching an acceptable model with a small value of errors. The step size is very significant in controlling the learning procedure as well as its decrease and increase rates, specifically, the behavior of errors increasing and decreasing. Table 2 shows the default and used values of these parameters.

Table 2. The main training parameters.

Parameter	Default	*genfis*1	*genfis*2	*genfis*3
Training epoch number	10	20	20	20
Training error goal	0	0	0	0
Initial step size	0.01	0.03	1.3	0.03
Step size decrease rate	0.9	1.5	1.5	1.5
Step size increase rate	1.1	1.5	1.5	1.5

3.1. Comparative Analysis of FIS Generation Methods in ANFIS

3.1.1. Grid Partitioning Method: Analysis of *genfis*1 Results

In an ANFIS, there are several approaches to creating the required members. A grid partition method (named in MATLAB as *genfis*1) is a widely used approach, such as in predicted and controlled PID's proportional gain (Kp) values [53]. A grid partition depends on the principle of the regular partitioning of data space in dividing the input data into memberships, and it divides the data with an equal step between the upper and lower limits, according to the number required by the user [54,55]. However, the current model automatically generated 25 rules using five memberships for each input. Later, a neural network is used for data training to estimate the best factors of memberships that can achieve the best agreement of the predicted ANFIS model concerning the tested data that enable the agreement between the test and the values predicted by the ANFIS. Figure 8 displays the membership functions of the inputs before and after training using *genfis*1. This in turn leads to the formation of rules with the number of the member's product for the first input and the member for the second input. Therefore, the conditions in this method will be 25, as in Figure 9. The rule base of *genfis*1 in detail and in the form of conditions is presented in Appendix A.

After training the scheme and creating rules that cover most of the expected cases, the approach was assessed using selective data to match it with the extracted result. The results proved the method's accuracy in estimating the output's true value, which is represented by the proportional gain of the PID controller (Kp), as in Figure 10a. The ANFIS method's ability to deal with computation operations and mathematical models led to a significant reduction in error, as shown in Figure 10b.

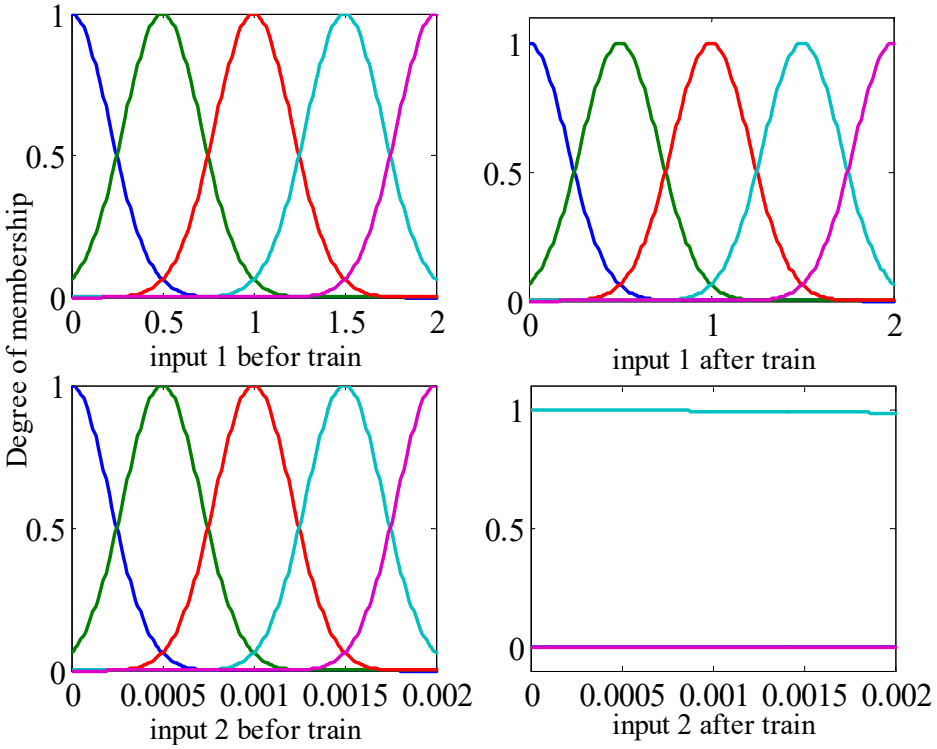

Figure 8. Inputs of membership functions before and after training using *genfis*1. The unit of measuring input 1 (position error) is cm; that for input 2 (derivative of error) is cm/s. The degree of membership is dimensionless.

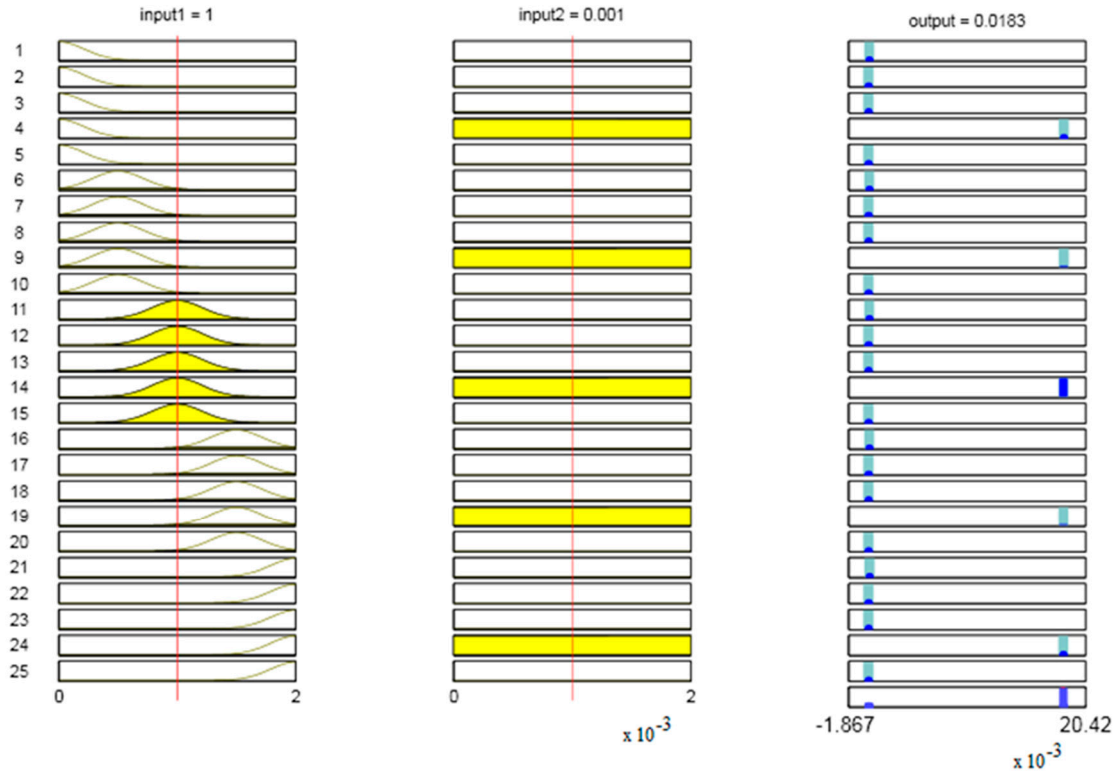

Figure 9. Rule base of *genfis*1.

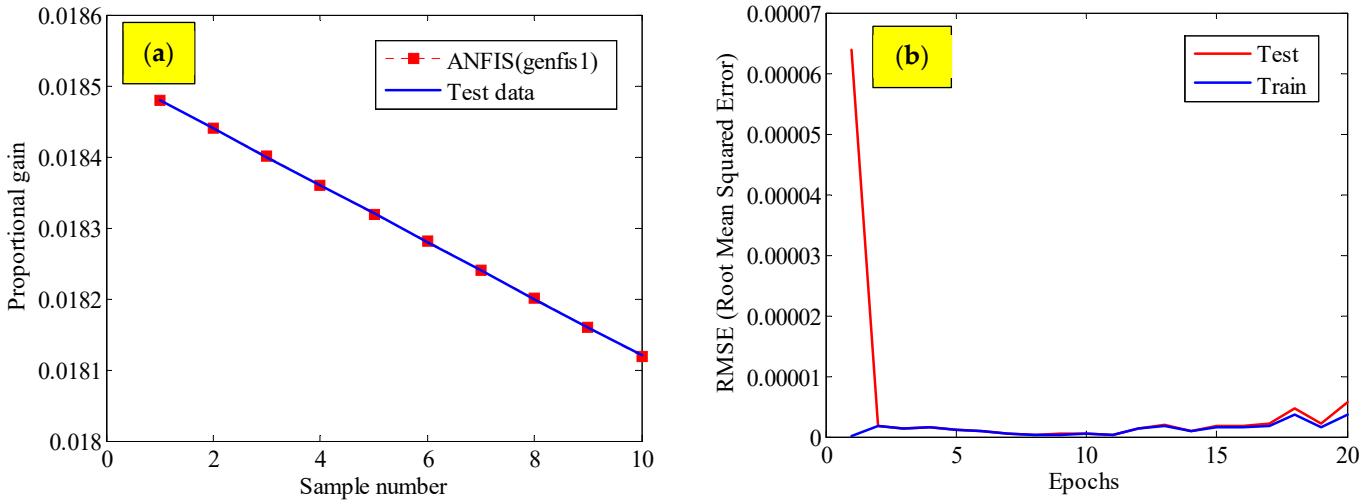

Figure 10. ANFIS *genfis*1: (**a**) prediction test, (**b**) root-mean-squared error (training and testing).

The surface plot of input–output in *genfis*1 is presented in Appendix A.

3.1.2. Subtractive Clustering Method: Evaluation of *genfis*2 Outcomes

To predict and control the second factor of PID, which is the integral gain (Ki), another method of constructing the ANFIS was used, which is the subtractive clustering method, which depends on dividing the data according to a radius that represents the extent of influence on the clusters [56,57]. This method is called *genfis*2 in MATLAB. Choosing a small radius means obtaining a large number of clusters, while choosing a large radius leads to obtaining a small number of clusters and, thus, a small number of memberships. However, a radius of 0.9 was chosen, which led to obtaining three memberships for each input. These memberships were trained to obtain the best factors using the combination

of backpropagation and the least-squares method, as shown in Figure 11. This method generates rules related to the generated clusters. Thus, the rules will be according to the number of clusters produced, which in this study were three, as shown in Figure 12. The rule base of *genfis*2 in detail and in form of conditions is presented in Appendix B.

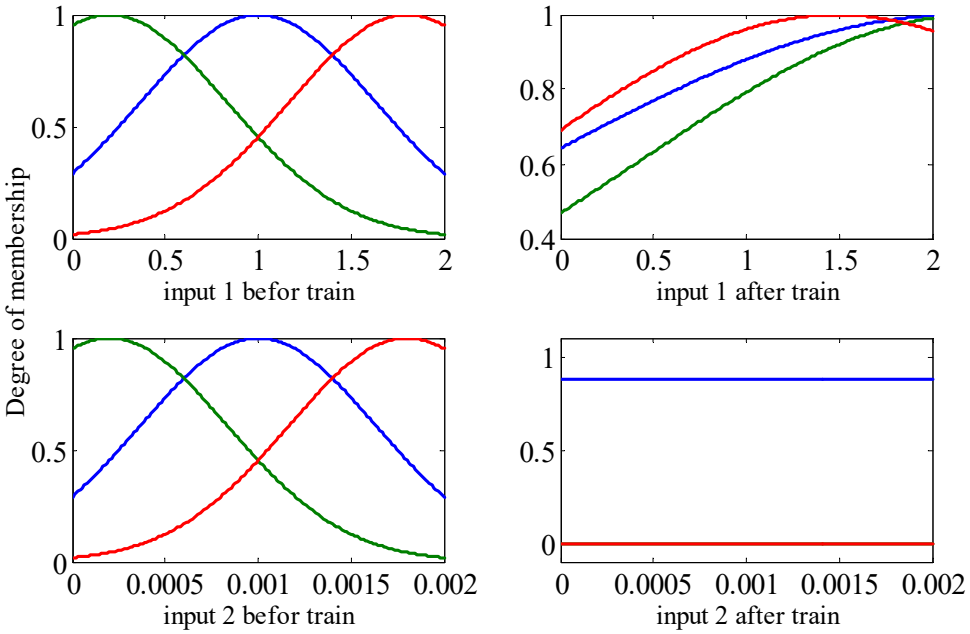

Figure 11. Input membership functions before and after training using *genfis*2. The unit of measurement for input 1 (position error) is cm; that for input 2 (derivative of error) is cm/s. The degree of membership is dimensionless.

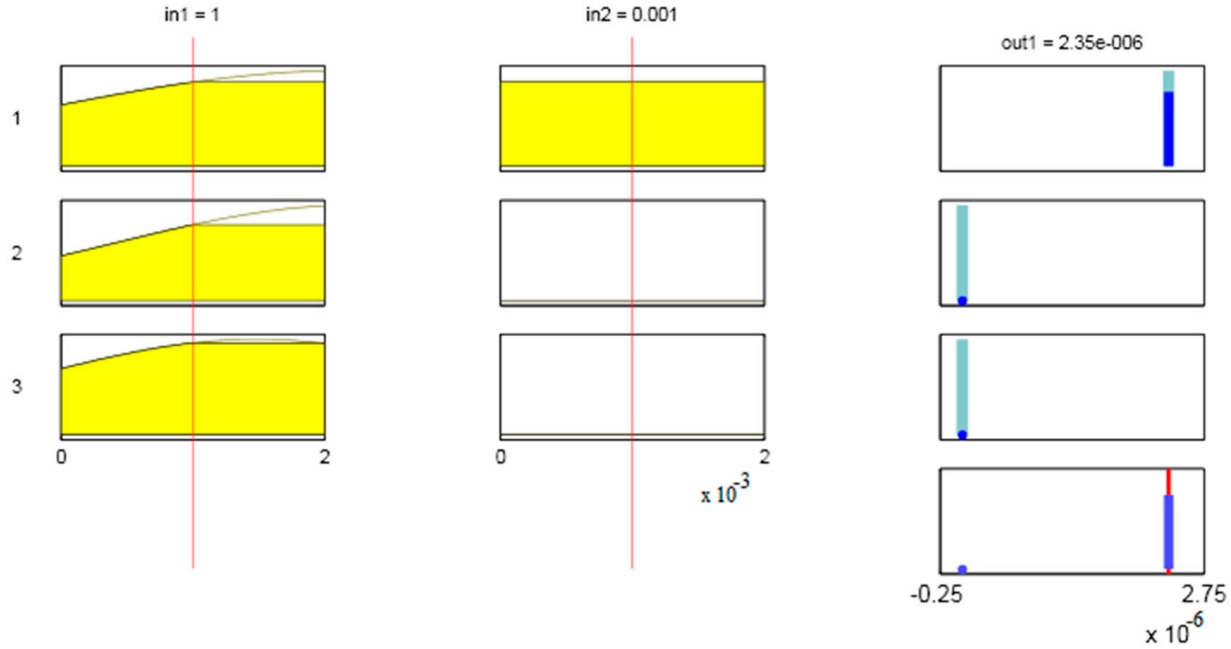

Figure 12. Rule base of *genfis*2.

The high ability of the ANFIS to form relationships between the input and output data, even with little experience in determining the behavior of these data, led to perfectly accurate results through complete agreement between the result extracted by *genfis*2 and the examination data, as in Figure 13a. The excellent ability of the ANFIS to form

a continuous surface and the ability to form mathematical models even with data with complex behavior led to a reduction in the error to a minimal value [58], as in Figure 13b.

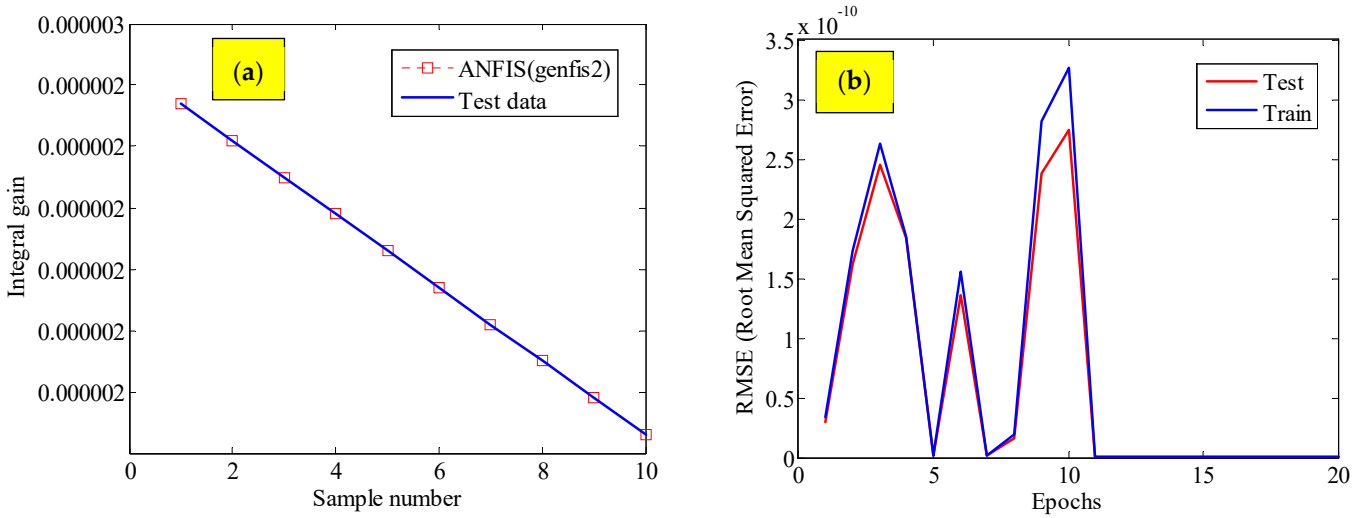

Figure 13. ANFIS *genfis*2: (**a**) prediction test, (**b**) root-mean-squared error (training and testing).

The surface plot of input–output in *genfis*2 is presented in Appendix B.

3.1.3. Fuzzy C-Means Clustering Approach: Results from *genfis*3

To control the derivative part (Kd) of the PID, the Fuzzy C-means clustering method (named *genfis*3 in MATLAB) was adopted, which depends on the user estimating the number of clusters [53]. After determining the number of required clusters, the method guesses the centers of these clusters, which often need to be corrected. After the initial guess, an objective function is determined that represents the minimum distance of the data from the centers of the guessed clusters until it reaches the best division of the clusters [59]. This method helps users of these applications divide their data into an appropriate number of members in case they need more experience sorting data that may contain strange and random values. However, four clusters were chosen in this study. They were trained sufficiently to obtain member functions with appropriate parameters that represent the true relationship between the input data and the output, as in Figure 14. The number of rules in this method is related to the number of clusters produced, so the number of rules was four, as in Figure 15. The rule base of *genfis*3 in detail and in the form of conditions is presented in Appendix C.

Data collection covering all expected changes in error is essential. Also, sorting the data in a way that diagnoses the correct mathematical relationship between the inputs and the output, and the accuracy of training led to highly accurate results in this method. Compared to the test data in Figure 16a, the result of genfis3 was perfectly accurate. Proper training and checking of the ANFIS before entering it into operation eliminates the errors accompanying the system's operation in the dynamic model [60,61]. As seen in Figure 16b, obtaining a small error during training is evidence of the method's efficiency in the future when it enters operation in the model designed for the robotic gripper arm.

The surface plot of input–output in genfis3 is presented in Appendix C.

After training all the methods used in the ANFIS, the proposed controller in this research is linked with the model designed for the arm grip, as in Figure 17. In order to make the required comparisons with the models and methods presented in previous research, the proposed model in the previous research was placed side by side with the current model to prove the efficiency and effectiveness of the presented controller. In this

model, the controller receives the error in the required gripper movement and its derivative. Each part of the controller determines the appropriate value to modify the three PID factors, where $genfis1$ modifies the value of (Kp) and $genfis2$ modifies the value of (Ki). In contrast, (Kd) is modified by $genfis3$.

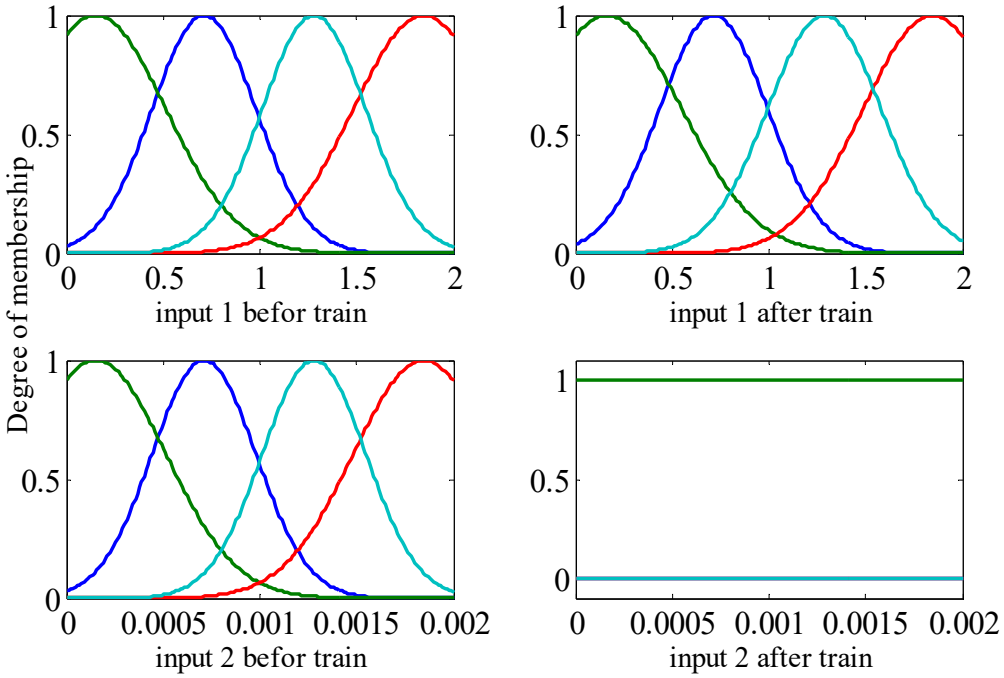

Figure 14. Input membership functions before and after training using $genfis3$. The unit of measuring input 1 (position error) is cm; that for input 2 (derivative of error) is cm/s. The degree of membership is dimensionless.

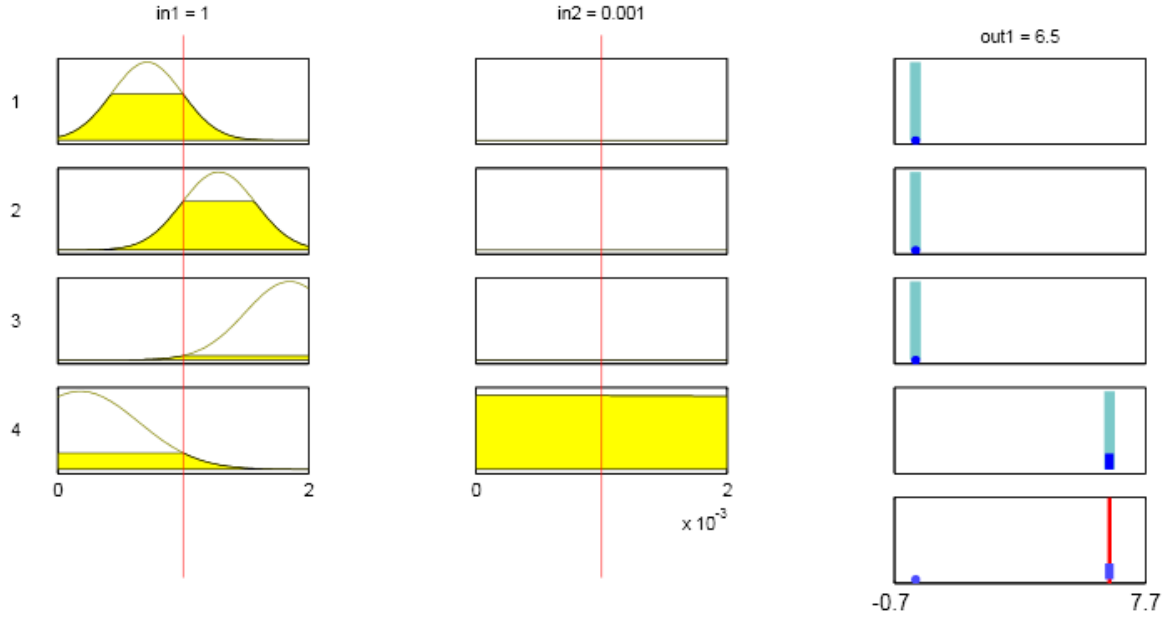

Figure 15. Rule base of genfis3.

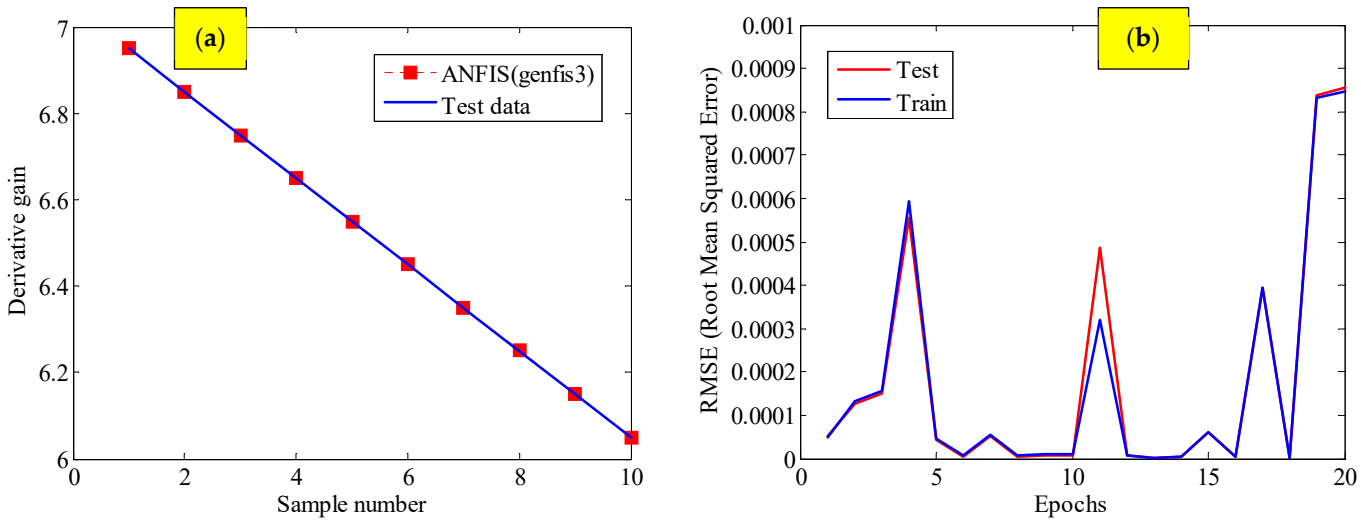

Figure 16. ANFIS genfis3: (**a**) prediction test, (**b**) root-mean-squared error (training and testing).

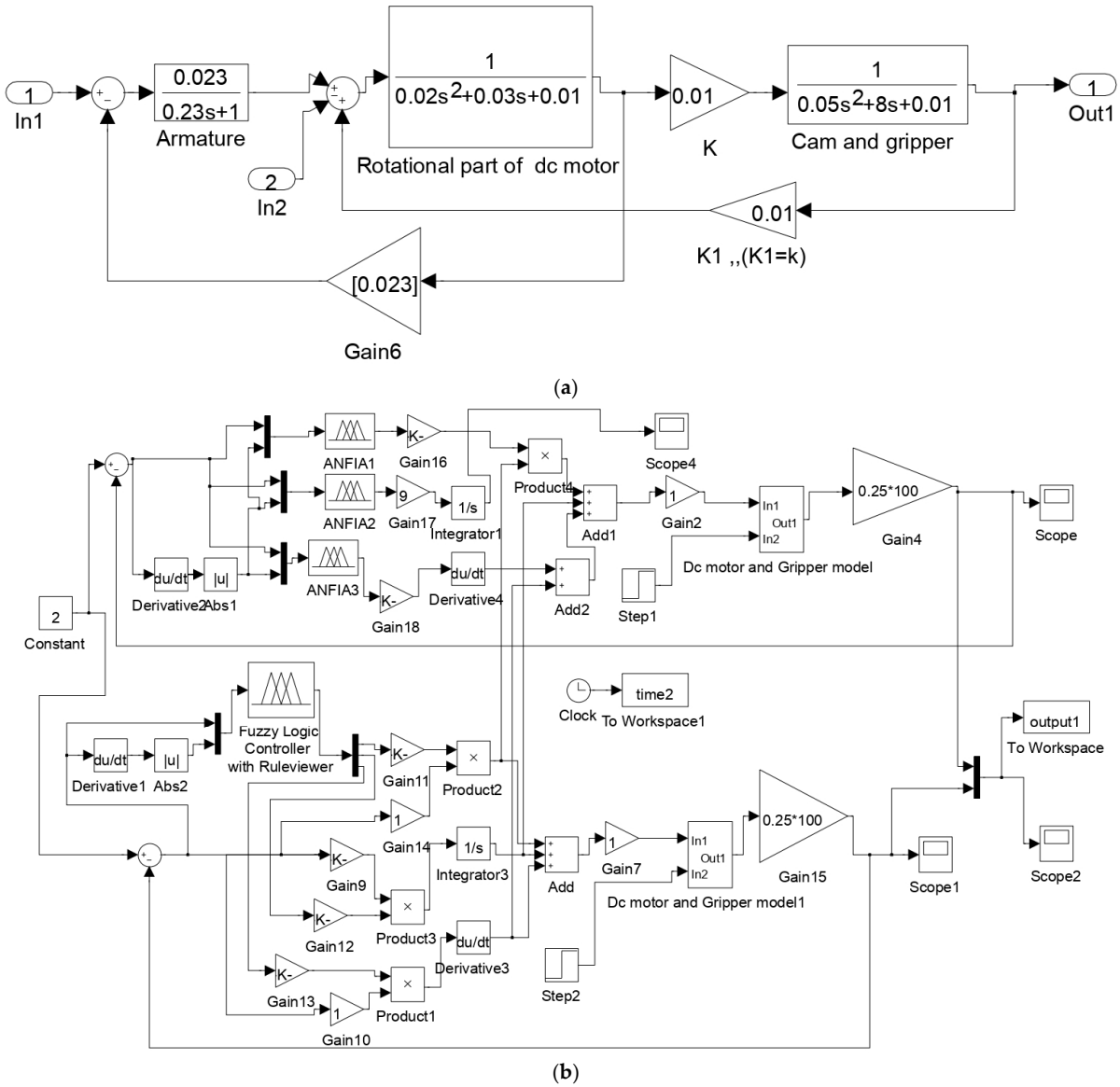

Figure 17. (**a**) The Simulink model of the system (motor, cam, and gripper). (**b**) Applying the proposed ANFIS for gripper position control.

To test and assess the efficiency of the controller presented in this study, a comparison was made with the controller's performance presented by [27], which used fuzzy logic to tune the PID factors. Also, the comparison was conducted with the traditional PID in MATLAB, as indicated in Figure 18. Moreover, even though fuzzy logic is suitable for human input and is acceptable to some of the control fields, the accuracy of the ANFIS method in dealing with mathematical analyses and ensuring a continuous output surface led to superior results compared to other controllers. When examining the results either in Figure 18 or Table 3, the rise time, which represents the time needed to reach the required value, was 76 s for the developed controller compared with the longer times for the other controllers. There is no doubt that this result is considered one of the required objectives in the precise operations and in the movement of the robot gripper for carrying out time-sensitive tasks without delay. Also, the overshoot could have been longer due to the satisfactory prediction of the derivative gain value, while it was 10 percent in the conventionally tuned PID. However, fuzzy logic may be able to eliminate the overshoot through the accuracy of the construction of the conditions. However, it showed a more significant value in the steady-state error (0.0001); this may not be desirable in precision industries such as the manufacture of electrical circuits and the transfer of small parts by robotic arms.

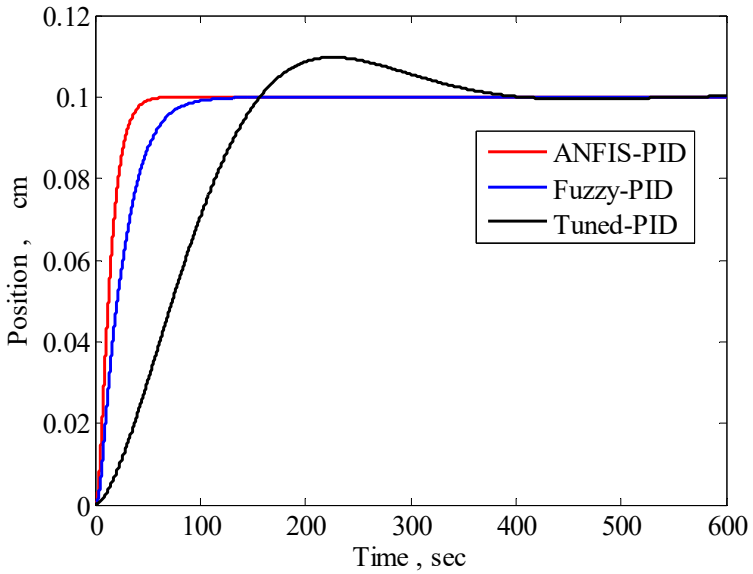

Figure 18. Position variation comparison between ANFIS-PID, Fuzzy-PID, and Tuned-PID controllers.

Table 3. Rise time, maximum overshooting, and steady-state error according to controller types.

Variable	Tuned PID	Fuzzy-PID	ANFIS-PID
Rise time (s)	156.93	150	76
Maximum overshoot (%)	10%	0	0
Steady-state error (cm)	0.0005	0.0001	0.000025

3.2. Effects of External Disturbances

Dynamic models may be subjected from time to time to certain disturbances, so the proposed controller was tested by applying a step disturbance to the model, as in Figure 19a. It is noticeably clear from the curve that the other controllers were significantly affected during the step time (200 s) and even after it, with the presence of a continuous error in the required value. However, due to the automatically prepared rule base, the controller presented had the ability to adjust the values of its parameters automatically to

resist the applied disturbance and maintain the required value of the gripper movement. Precise movement is essential in some applications, such as placing electrical resistors and transistors in their correct positions in electrical circuits before soldering them. Regarding the traditional and fuzzy logic controllers, the extensive range in determining the output value related to the output membership area in the controller construction may lead to a difference from the required values. The ANFIS-PID controller was tested in determining a precise displacement movement of 0.05 cm, and the result shown in the curve in Figure 19b proves the accuracy of the method compared to Fuzzy-PID because it deals with an output with a continuous and precise data surface with memberships that are either linear or constant. Also, the accuracy of forming the mathematical relationship between the input and output data by taking advantage of the neural skills in training and prediction was the reason for obtaining a precise displacement with a fast arrival time.

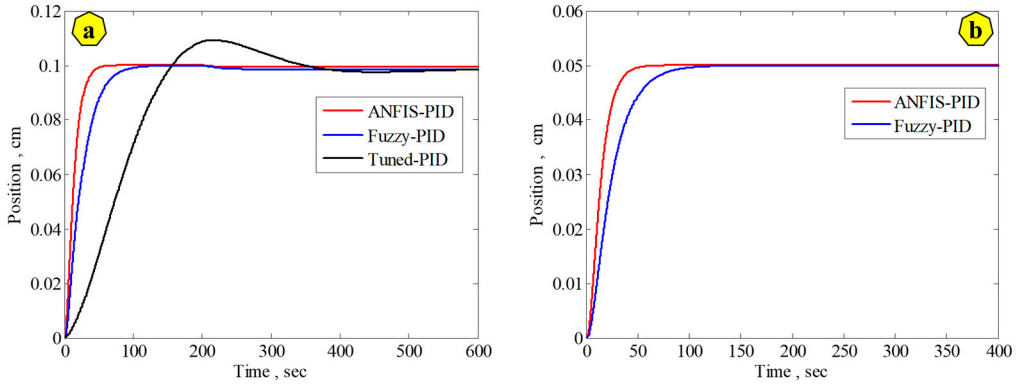

Figure 19. (**a**) Effect of disturbance on the ANFIS-PID, Fuzzy-PID, and Tuned-PID controllers, (**b**) precision movement of gripper during ANFIS-PID and Fuzzy-PID controllers.

3.3. Effects of Displacement Variation on ANFIS Model

In robotic gripper controllers, it is necessary to ensure the controller's flexibility in dealing with various displacements required to perform different tasks. Therefore, the developed controller was tested for different displacement values, as shown in Figure 20. Three displacements were examined to cover all the required gripper movements' ranges: 0.05 cm (small), 0.5 cm (medium), and 1.5 cm (large). The developed controller showed the same accuracy and efficiency in controlling different displacements by correctly and instantly tuning the PID values (Kp, Ki, and Kd). The performance showed a fast rise time with an overshoot and a steady-state error approaching zero. This skill enables the robot gripper to hold very fine samples with different size gradations. The controller (ANFIS-PID) possessed the neural ability to make predictions and the fuzzy strength to make decisions.

The variations in the main parameters of the dynamic model, such as rotating mass and damping coefficient, are considered extremely dangerous, especially for the rotating parts. However, the effect of increasing the moment of inertia of the rotating parts in the electric DC motor that operates the robot's gripper has been tested. This change dramatically affects the system's oscillation because it relates to an integral part of the model. This change will increase the overshoot and settling time, which requires fast adaptation in the value of the controller's integral gain (Ki) and an instant increase in the derivative gain (Kd). The result shown in Figure 21 proves the acceptable performance of the developed ANFIS-PID controller compared to Fuzzy-PID despite the presence of a relatively small overshoot because the test was challenging. The overshoot is very small and can be neglected. Therefore, it cannot affect the accuracy of the positioning. Figure 21 shows the efficiency of the ANFIS-PID controller in terms of quickly reaching the required value for the location with a rise time of 30 s compared to the Fuzzy-PID method, where

the time was relatively long (120 s). This advantage comes from the accurate prediction of the main factors of PID, which leads the actuator to the correct direction to move the grip at the appropriate speed. Also, the overshoot was relatively small (1.3% of set point 0.1 cm), and the error was close to zero.

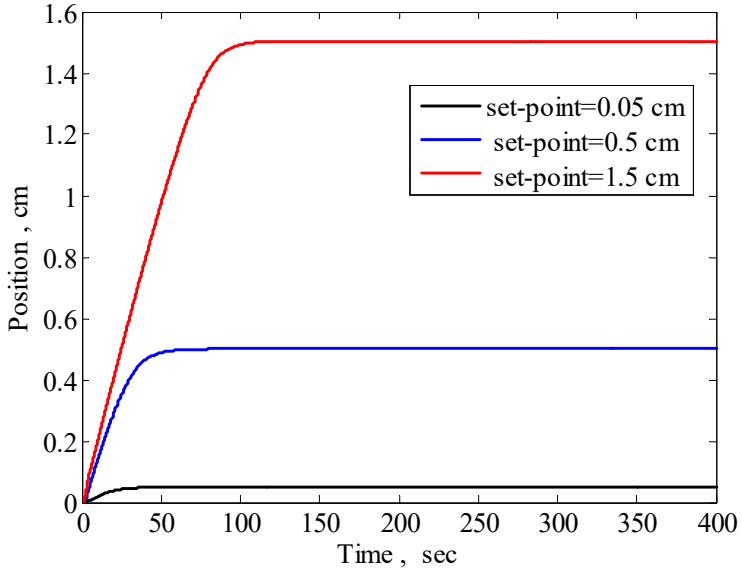

Figure 20. Testing of developed ANFIS-PID controller at different set points.

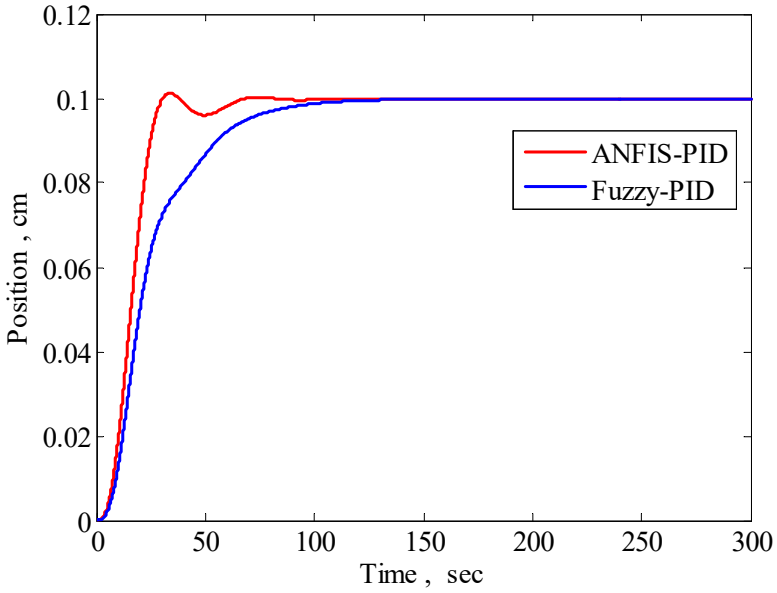

Figure 21. Precision movement of the gripper in the developed ANFIS-PID and Fuzzy-PID controllers.

Position control is essential to the gripper or the hand of the robot, allowing for more advanced manipulation, managing the position of the fingers, and generating a smooth trajectory [1,62,63]. The following section presents and develops simulations with grip force control.

4. Gripper Force Control Simulations and Results

The grip force control simulations and results are presented and discussed in this section. Grip force control is based on the motor current and measures the grip force directly. Controlling the force in a robot arm's grip is an especially important topic due to its effectiveness in safely transferring samples, pieces, objects, and varied materials. The

grip force control is implemented using the proposed ANFIS-PID system and is tested and evaluated with different cases and scenarios, which are (1) achieving a required force of 30 N, (2) changing the required force from 30 N to 60 N, and (3) decreasing the required force to 0 N. In addition, the performance of the proposed controller is compared with other methods, such as the Fuzzy-PID controller.

The analysis of the force representation on the proposed and designed gripper is shown in Figure 22. The appropriate grip force in the presented model must equal the spring force and the reaction force that ensure that the sample or the object does not slip, obtained from the following equations based on Figure 22.

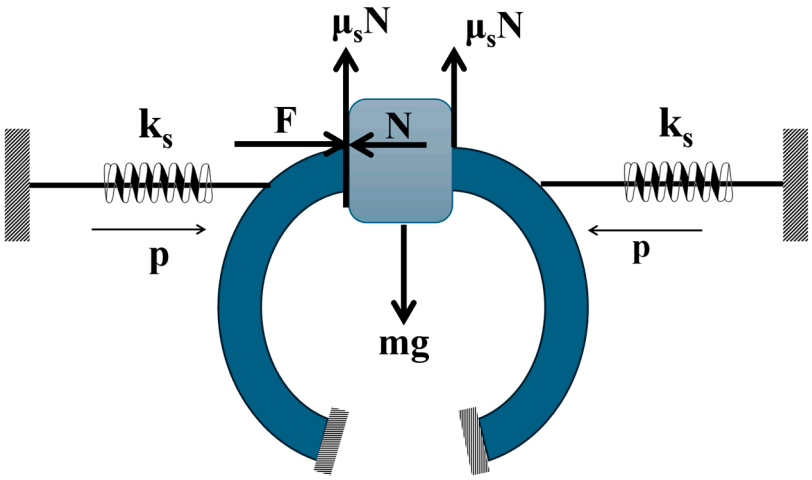

Figure 22. A mathematical model of force representation on the proposed gripper.

The sum of forces in the $x-$ direction is equal to zero; therefore,

$$\sum F_x = 0 \tag{19}$$

Therefore, for one segment of the gripper,

$$F = K_s p + N \tag{20}$$

where F is the grip control force at one part of the gripper, K_s is the spring constant, p is the displacement of the spring in the $x-$ direction or the position of the gripper, and N is the reaction force.

The sum of forces in the $y-$ direction is equal to zero; therefore,

$$\sum F_y = 0 \tag{21}$$

Therefore,

$$mg = 2\mu_s N \tag{22}$$

where m is the mass of the object, g is the acceleration of gravity, and μ_s is the coefficient of friction between the gripper and the sample or object.

The reaction force N can be obtained from Equation (22), as follows:

$$N = \frac{mg}{2\mu_s} \tag{23}$$

Substituting Equation (23) into (20) results in the following:

$$F = K_s p + \frac{mg}{2\mu_s} \tag{24}$$

For safety, the total control force equal to 2F is as follows:

$$\text{The total control force } \geq 2K_s p + \frac{mg}{\mu_s} \tag{25}$$

The Simulink model used for implementing the grip force control is presented in Figure 23. Figure 23a represents only the application of the proposed ANFIS-PID on the system. Figure 23b represents the application of the proposed ANFIS-PID and the Fuzzy-PID on the system to compare their performance simultaneously. In addition, the values of the main parameters used in this simulation are presented in Table 4.

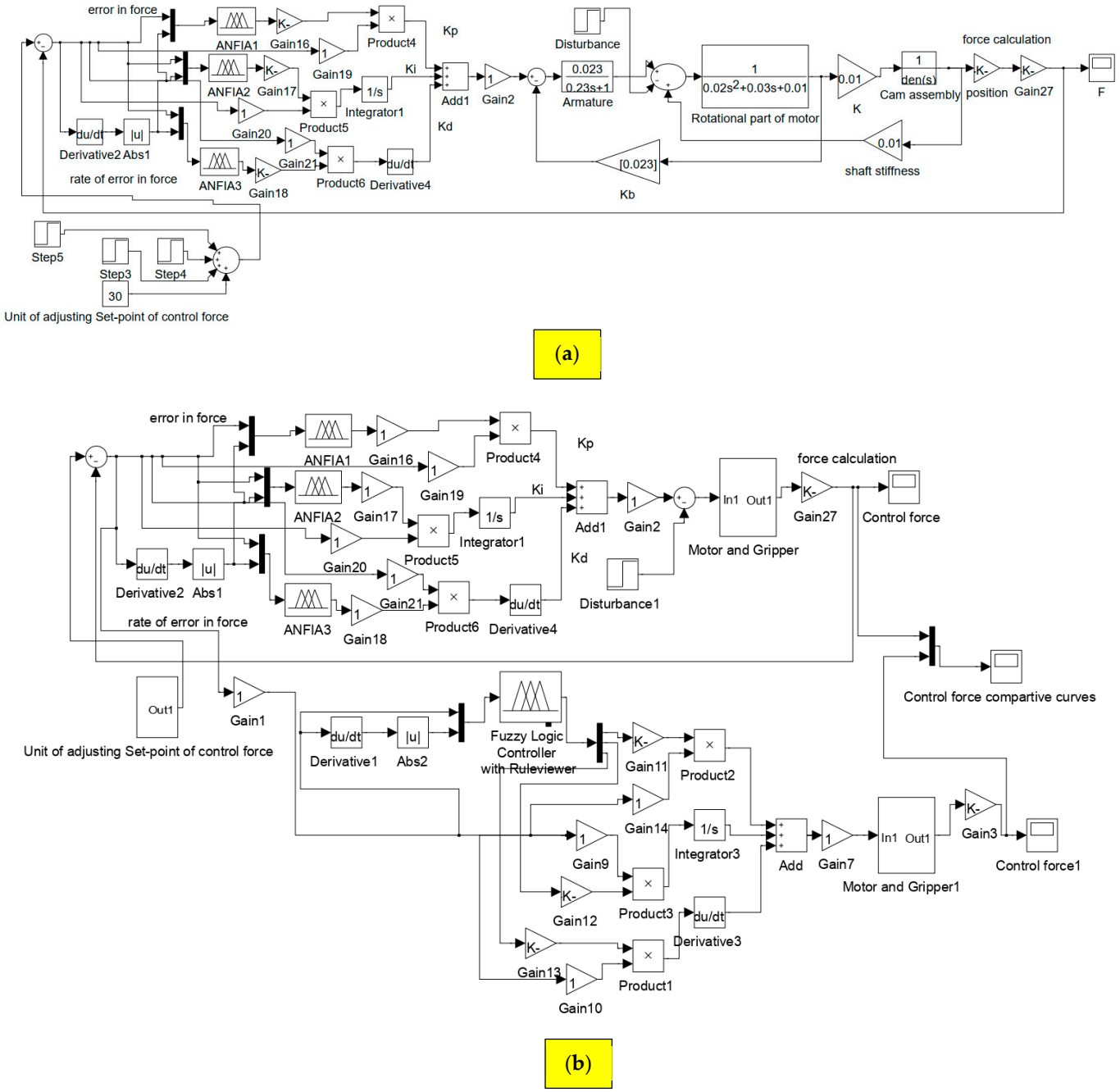

Figure 23. The Simulink model is implemented to control the gripper force. (**a**) Applying only the proposed ANFIS-PID to the system. (**b**) Applying the proposed ANFIS-PID and the Fuzzy-PID to the system for performance comparison.

Table 4. The values of the main parameters used in the simulation of force control.

Parameter	Magnitude
K_s	8–30 KN/m
m	0.2–5 kg
μ_s	0.2–0.8
b_1	0.03 N·m·s
b_2	8 N·m·s
J_1	0.02 kg·m^2
J_2	0.05 kg·m^2
Motor constant, Km	0.023 N·m/A
Back electromotive gain, Kb	0.023 V/rad
La	0.23 Henry
r	3.5 cm
Ra	1 Ω

4.1. Scenario 1: The Ability to Achieve a Required Force of 30 N to Hold an Object

The required force (set point) is determined based on the weight of the specimen to be moved and the position of the grip that must be achieved. To achieve a position of 0.1 cm, the mass to be moved is selected, which ranges between 0.5 and 5 kg and the value of the spring constant is determined, which ranges between 8–30 and KN/m. The grip's ability to achieve a force of 30 N in 75 s was tested, as shown in Figure 24. The result from Figure 24 shows the extent and the achievement of stability in the force after the decision to hold the sample/object and before that. This shows the high performance of the proposed ANFIS-PID.

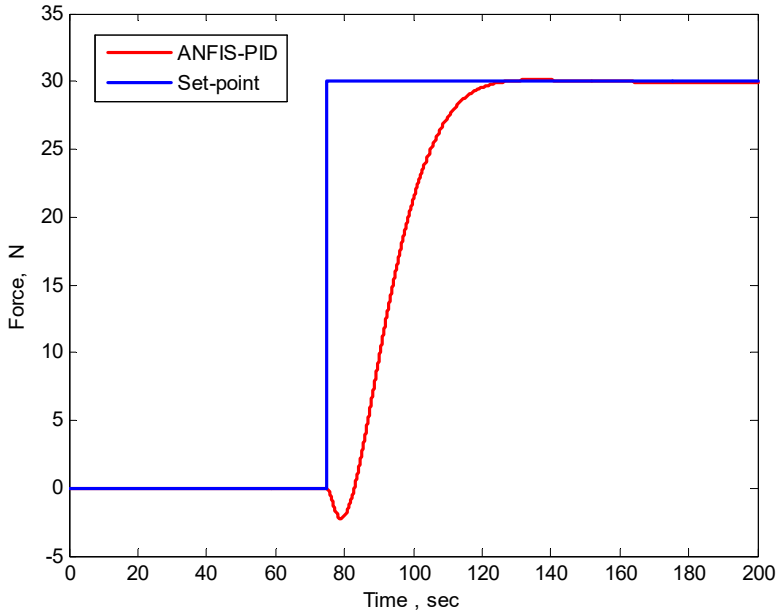

Figure 24. Force control by the proposed ANFIS-PID to achieve a required force (set point) of 30 N.

The result of the presented ANFIS-PID model is compared with the Fuzzy-PID method, as shown in Figure 25. From Figure 25, with the Fuzzy-PID controller, there is a clear difference in accuracy, a clear disturbance at the beginning of the decision, and a noticeable delay in the rise time method. There are many reasons for the decline in the strength of the Fuzzy-PID method, including the range in the memberships and their numbers, which causes a decision not to be taken accurately sometimes, as well as experience in writing the

conditions. As seen in the figure, the performance of the proposed ANFIS-PID is higher and desirable.

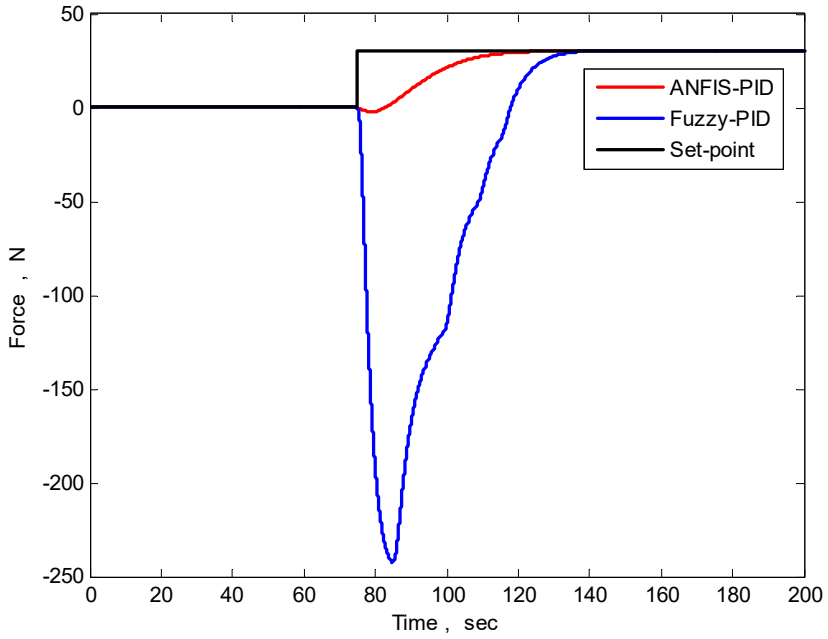

Figure 25. The performance comparison between the proposed ANFIS-PID and the Fuzzy-PID in controlling a required force of 30 N (set point).

4.2. Scenario 2: Changes in the Required Force from 30 N to 60 N During the Holding an Object

The gripper can hold and transfer some pieces, samples, or objects that require a change in the holding force, such as soft materials or materials whose direction of transfer changes. Therefore, the component of the friction force changes. This system is tested as shown in Figure 26. The proposed ANFIS-PID shows a clear recovery from the change in force and maintains the system's stability at the value of the new force (60 N).

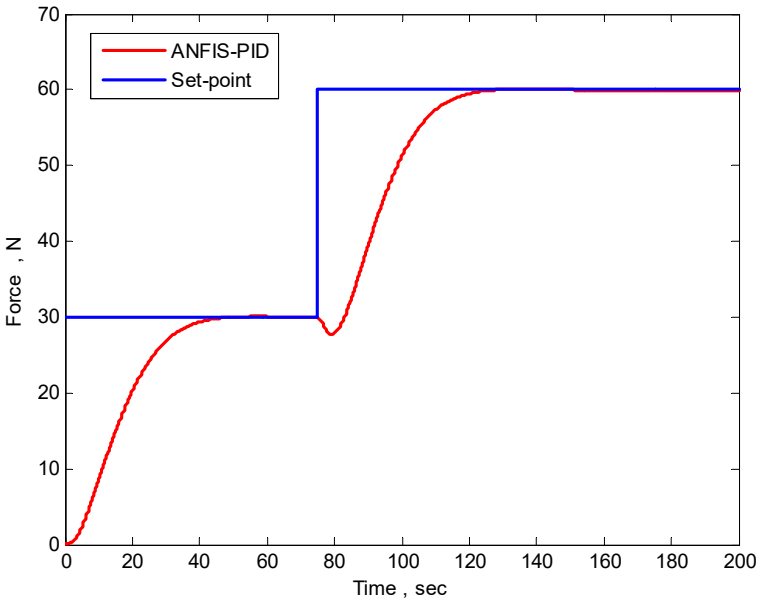

Figure 26. The performance of the proposed ANFIS-PID control using two set points of forces or, in other words, when there is change in the required force from 30 N to 60 N.

The proposed ANFIS-PID is compared with the Fuzzy-PID method, as presented in Figure 27. The result from this comparison shows that, with the Fuzzy-PID method, confusion is observed at the beginning of the transition from the current grip force (30 N) to the new force (60 N) as well as the presence of a clear overshoot and a delay in the stability of the force. From this comparison, the performance of the proposed ANFIS-PID is better and is desirable. The speed of bringing the controlling force to its specified value is considered one of the important things in the work of the robot grip in avoiding any issues with holding the sample correctly. In any case, as seen in Figure 27, it is noted that the proposed ANFIS-PID controller achieved the required force in a rise time of 49 s, which is a suitable time compared to the method of Fuzzy-PID, which took a rise time of 75 s.

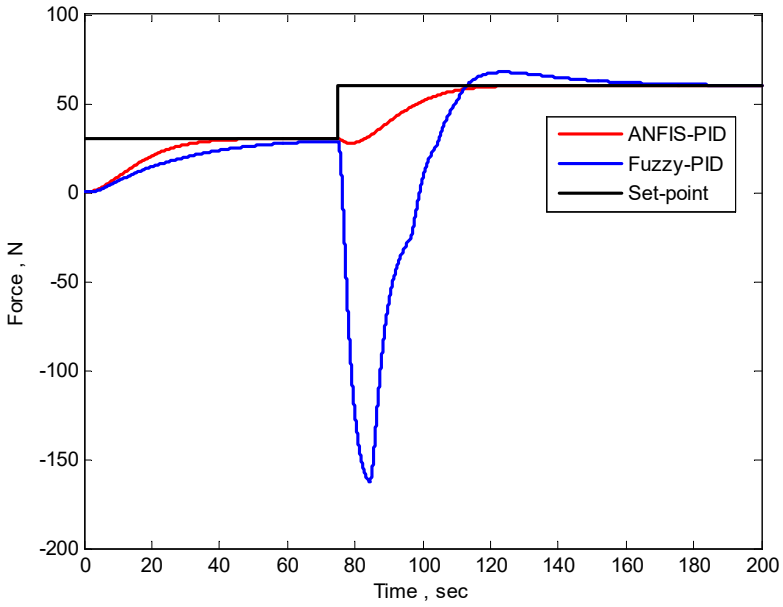

Figure 27. The performance comparison of the proposed ANFIS-PID and the Fuzzy-PID using two set points of forces or when there is a change in the required force from 30 to 60 N.

4.3. Scenario 3: The Force Is Dropped to 0 N (The Gripper Is Returning to the Original Position)

In most cases, the robot gripper may succeed in holding the sample/object but fail to release it safely. The proposed ANFIS-PID model is tested when its grip returns to the original position and the force drops to zero. This case is presented in Figures 28 and 29. From these figures, the efficiency of the proposed ANFIS-PID method in the case of the force rising and falling is higher than that of the Fuzzy-PID method. The Fuzzy-PID method shows a clear delay, particularly at the moment of descent.

From the results of these three different scenarios, the proposed ANFIS-PID has better and desirable actual gripping performance of objects. Therefore, the proposed ANFIS-PID can work efficiently under different conditions. The performance of the proposed controller in controlling force is in complete agreement with many previous research works, such as the research work of Sadun et al. and Vitrani et al. [64,65].

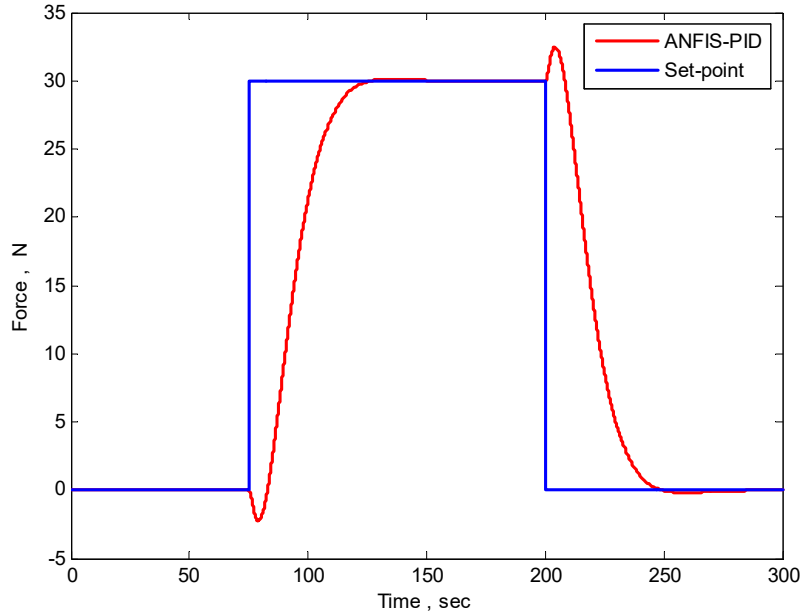

Figure 28. Force control by the proposed ANFIS-PID when the set point drops from 30 N to 0.

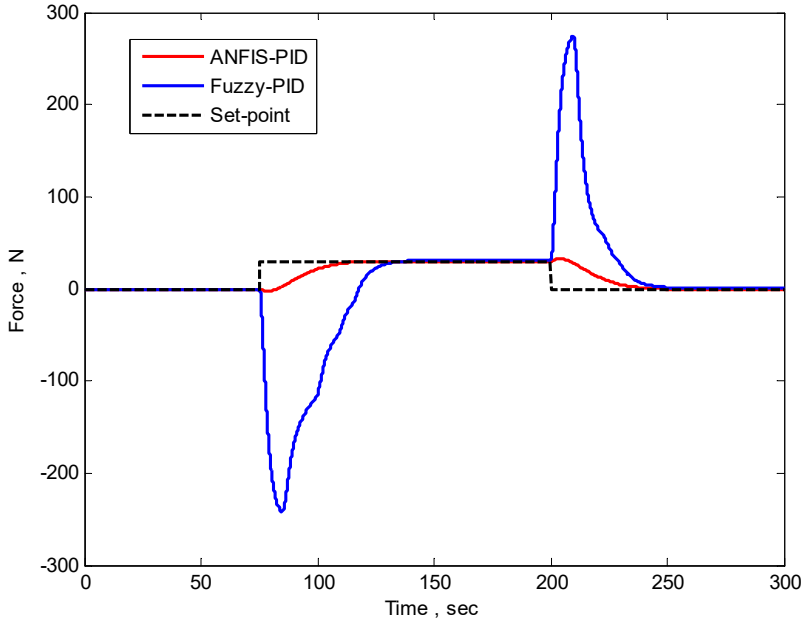

Figure 29. The comparison between the proposed ANFIS-PID and the Fuzzy-PID when the set point drops from 30 N to 0.

4.4. Effects of Internal and External Disturbances

To test the proposed controller's ability to overcome internal and external disturbances that the system may be exposed to, an external disturbance was imposed at time 100 s and an internal disturbance at time 120 s, as shown in Figure 30. It is noted from the figure that the controller was able to compensate for the deficiency in the required force in the event of an external disturbance. Also, despite the difference in the nature of the internal disturbances being positive, the controller showed high efficiency in reducing this excess force and returning the force curve to the required/desired force, which provides stability in controlling the samples in a flexible and accurate manner. Also, the maximum overshoot was almost non-existent, and the rise time was very satisfactory (approximately 45 s).

The executed codes implemented in this paper are attached as Supplementary Material to this paper.

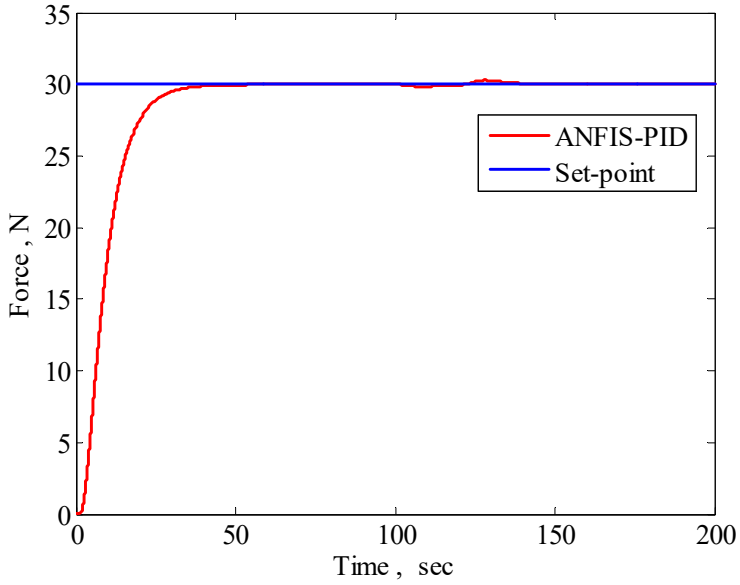

Figure 30. Testing the ability of the proposed controller to overcome internal and external disturbances.

5. Conclusions and Future Work

Designing a robotic gripper and finding the best ways to control its motion is an essential goal in the industry. This study developed a robotic gripper design by adding a cam to improve the motion and develop the gripping mechanism effectively. In addition, position and grip force control models based on ANFIS-PID were developed. The three methods, grid partitioning $genfis1$, subtractive clustering $genfis2$, and fuzzy C-means clustering $genfis3$, were used in the tests within MATLAB Simulink. The results were compared with Fuzzy-PID and traditional tuned-PID controllers. The following are the main conclusions:

1. The added cam improved gripping strength, and the ANFIS model effectively handled rise time and supported settling time.
2. Compared to Fuzzy-PID and conventional tuned-PID controllers, the developed ANFIS-PID controller demonstrated more efficient performance. This performance improvement was evident in all the scenarios tested, including grid partitioning ($genfis1$), subtractive clustering ($genfis2$), and fuzzy C-means clustering ($genfis3$).
3. When the developed ANFIS-PID controller was examined under the influence of dynamic disturbance, it could automatically adjust the values of its parameters to resist the applied disturbance and maintain the required value of the gripper movement.
4. The developed ANFIS-PID controller was very flexible when dealing with variable displacements and a wide range of set points. Although it was tested at low values of 0.05 cm, medium values of 0.5 cm, and relatively large values of 1.5 cm, the results were encouraging, and a steady state was achieved quickly for various set points.
5. The result from developing grip force control by investigating three different scenarios reveals a higher actual gripping performance of objects when using the proposed ANFIS-PID than the Fuzzy-PID system.
6. The force controller's ability to overcome internal and external disturbances that the system may be exposed to was tested. The results show that the proposed controller presented high efficiency in reducing these disturbances and returning the force curve to the desired value, which provides stability in controlling the samples in a flexible and accurate manner.

The restriction of the proposed method is its application and investigation with the input of a step function. However, in future work, other input functions, such as ramp,

parabolic, and random functions, can be applied. Implementing the proposed design in real experiments will be considered in future work. Robust controllers such as H-Infinity can be applied, investigated, and compared with the current approach. Furthermore, other intelligent controllers, such as those that use different neural network-based controllers, can also be investigated.

Supplementary Materials: The following supporting information can be downloaded at: https://www.mdpi.com/article/10.3390/automation6010004/s1. The executed codes in this paper are attached and uploaded.

Author Contributions: Conceptualization, I.A.K., R.A.-S. and A.-N.S.; methodology, I.A.K., R.A.-S. and A.-N.S.; software, A.-N.S. and I.A.K.; validation, I.A.K. and A.-N.S.; formal analysis, I.A.K., A.-N.S. and R.A.-S.; investigation, I.A.K., R.A.-S. and A.-N.S.; resources, I.A.K., R.A.-S. and A.-N.S.; writing—original draft preparation, I.A.K., R.A.-S. and A.-N.S.; writing—review and editing, R.A.-S. and A.-N.S.; supervision, R.A.-S. and A.-N.S.; project administration, A.-N.S. and R.A.-S. All authors have read and agreed to the published version of the manuscript.

Funding: This research received no external funding.

Data Availability Statement: Data are contained within the article and Supplementary Materials.

Conflicts of Interest: The authors declare no conflicts of interest.

List of Used Symbols

Symbol	Definition	Measuring Unit
r	Radius of base circle of cam	cm
b_1	Damping coefficient of DC motor parts	N·m·s
b_2	Damping coefficient of cam assembly	N·m·s
θ1	Angular movement of rotating parts of DC motor	rad
θ2	Angular movement of rotating parts of cam assembly	rad
w	Angular speed of DC motor	rad/s
I_a	Armature current	A
Ra	Armature resistance	Ω
La	Armature inductance	H
T_L	Motor torque	N·m
J_1	Moment of inertia of rotating part of DC motor	kg·m^2
J_2	Moment of inertia of rotating part of cam assembly	kg·m^2
K	Stiffness constant of shaft	N·m/rad
Kp	Proportional gain of PID controller	------
Ki	Integral gain of PID controller	------
Kd	Derivative gain of PID controller	------
F	Control force	N
K_s	Spring constant	N/m
m	Mass of sample, piece, or object	kg
N	Reaction force	N
μs	Coefficient of friction between gripper and sample	------
g	Acceleration of gravity	m/s^2

Appendix A. Additional Information and Figures for *genfis*1

(A) Rule base of *genfis*1

In this rule base, ep represents the error in position, dep represents the derivative in the error, Kp represents the proportional gain of the PID controller, and RW represents the weight of the rule.

Rule base of *genfis*1
1. "If (ep is in1_mf1) & (dep is in2_mf1) then (Kp is out1_mf1) (RW)"
2. "If (ep is in1_mf1) & (dep is in2_mf2) then (Kp is out1_mf2) (RW)"
3. "If (ep is in1_mf1) & (dep is in2_mf3) then (Kp is out1_mf3) (RW)"
4. "If (ep is in1_mf1) & (dep is in2_mf4) then (Kp is out1_mf4) (RW)"
5. "If (ep is in1_mf1) & (dep is in2_mf5) then (Kp is out1_mf5) (RW)"
6. "If (ep is in1_mf2) & (dep is in2_mf1) then (Kp is out1_mf6) (RW)"
7. "If (ep is in1_mf2) & (dep is in2_mf2) then (Kp is out1_mf7) (RW)"
8. "If (ep is in1_mf2) & (dep is in2_mf3) then (Kp is out1_mf8) (RW)"
9. "If (ep is in1_mf2) & (dep is in2_mf4) then (Kp is out1_mf9) (RW)"
10. "If (ep is in1_mf2) & (dep is in2_mf5) then (Kp is out1_mf10) (RW)"
11. "If (ep is in1_mf3) & (dep is in2_mf1) then (Kp is out1_mf11) (RW)"
12. "If (ep is in1_mf3) & (dep is in2_mf2) then (Kp is out1_mf12) (RW)"
13. "If (ep is in1_mf3) & (dep is in2_mf3) then (Kp is out1_mf13) (RW)"
14. "If (ep is in1_mf3) & (dep is in2_mf4) then (Kp is out1_mf14) (RW)"
15. "If (ep is in1_mf3) & (dep is in2_mf5) then (Kp is out1_mf15) (RW)"
16. "If (ep is in1_mf4) & (dep is in2_mf1) then (Kp is out1_mf16) (RW)"
17. If (ep is in1mf4) & (dep is in2mf2) then (output is out1mf17) (RW)"
18. "If (ep is in1_mf4) & (dep is in2_mf3) then (Kp is out1_mf18) (RW)"
19. "If (ep is in1_mf4) & (dep is in2_mf4) then (Kp is out1_mf19) (RW)"
20. "If (ep is in1_mf4) & (dep is in2_mf5) then (Kp is out1_mf20) (RW)"
21. "If (ep is in1_mf5) & (dep is in2_mf1) then (Kp is out1_mf21) (RW)"
22. "If (ep is in1_mf5) & (dep is in2_mf2) then (Kp is out1_mf22) (RW)"
23. "If (ep is in1_mf5) & (dep is in2_mf3) then (Kp is out1_mf23) (RW)"
24. "If (ep is in1_mf5) & (dep is in2_mf4) then (Kp is out1_mf24) (RW)"
25. "If (ep is in1_mf5) & (dep is in2_mf5) then (Kp is out1_mf25) (RW)"

(B) The surface plot of input–output in *genfis*1

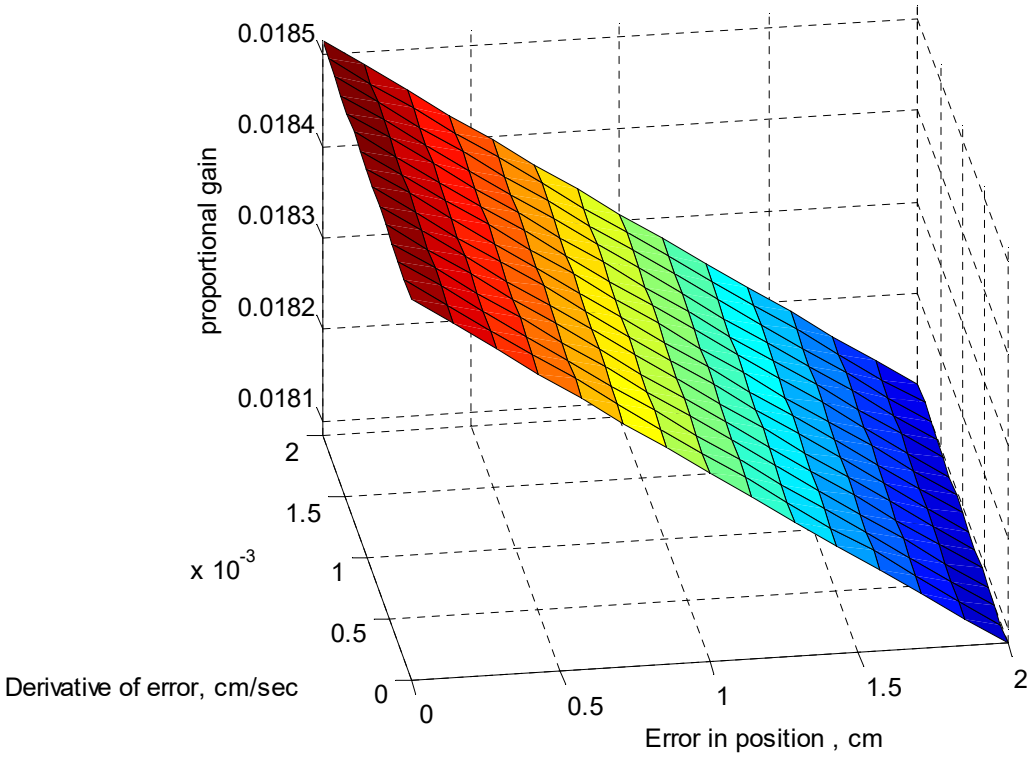

Figure A1. The surface plot of input–output in *genfis*1.

Appendix B. Additional Information and Figures for *genfis*2

(A) Rule base of *genfis*2

In this rule base, ep represents the error in position, dep represents the derivative in the error, Ki represents the integral gain of the PID controller, and RW represents the weight of the rule.

Rule base of *genfis*2
1. "If (ep is in1_cluster1) & (dep is in2_cluster1) then (Ki is out2_cluster1) (RW)"
2. "If (ep is in1_cluster2) & (dep is in2_cluster2) then (Ki is out2_cluster2) (RW)"
3. "If (ep is in1_cluster3) & (dep is in2_cluster3) then (Ki is out2_cluster3) (RW)"

(B) The surface plot of input–output in *genfis*2

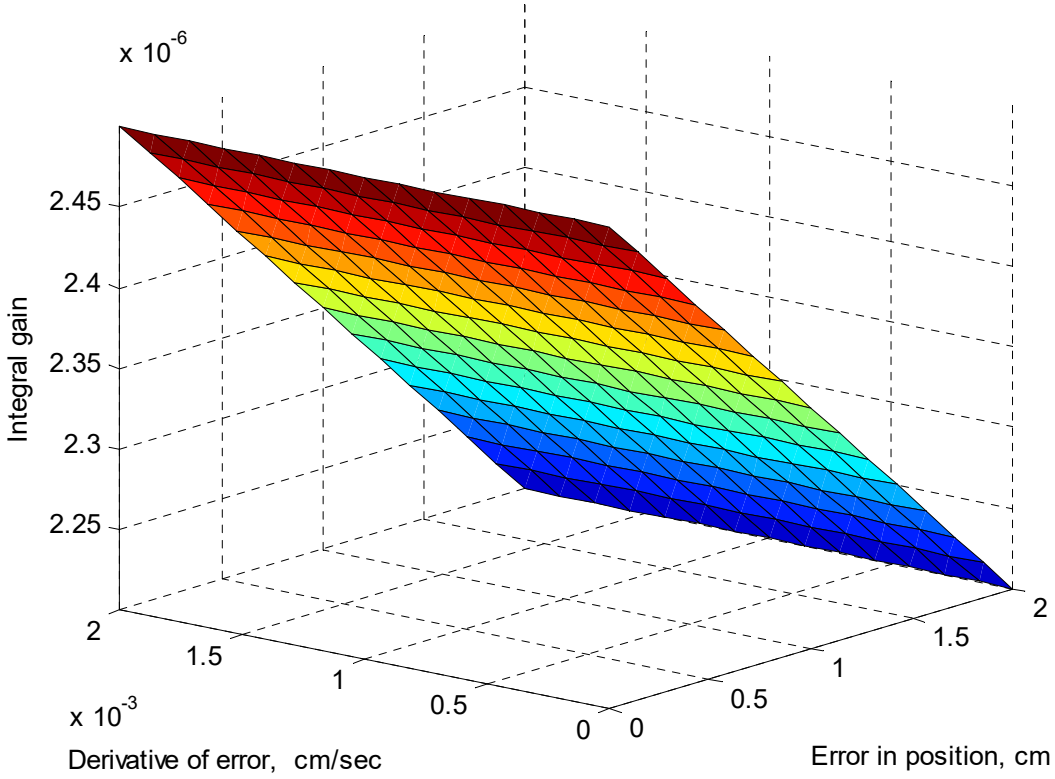

Figure A2. The surface plot of input–output in genfis2.

Appendix C. Additional Information and Figures for *genfis*3

(A) Rule base of *genfis*3

In this rule base, ep represents the error in position, dep represents the derivative in the error, Kd represents the derivative gain of the PID controller, and RW represents the weight of the rule.

Rule base of genfis3
1. "If (ep is in1_cluster1) & (dep is in2_cluster1) then (Kd is out3_cluster1) (RW)
2. "If (ep is in1_cluster2) & (dep is in2_cluster2) then (Kd is out3_cluster2) (RW)
3. "If (ep is in1_cluster3) & (dep is in2_cluster3) then (Kd is out3_cluster3) (RW)
4. "If (ep is in1_cluster4) & (dep is in2_cluster4) then (Kd is out3_cluster4) (RW)

(B) The surface plot of input–output in *genfis*3

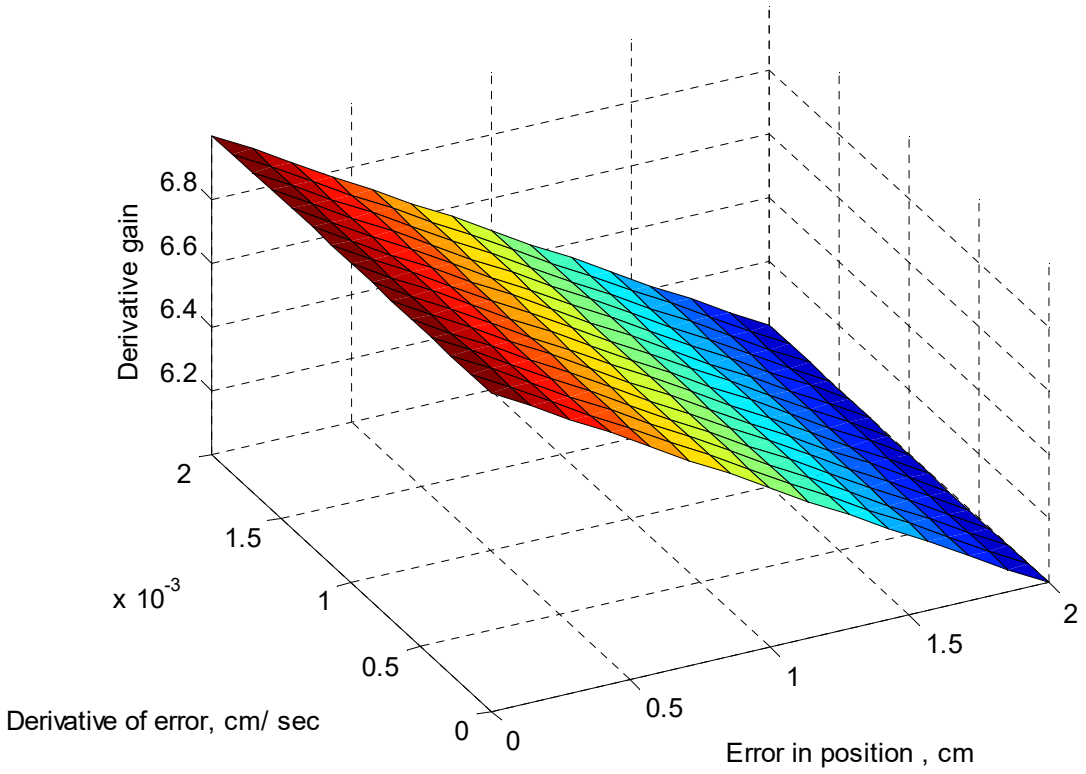

Figure A3. The surface plot of input–output in *genfis*3.

References

1. Zhang, B.; Xie, Y.; Zhou, J.; Wang, K.; Zhang, Z. State-of-the-art robotic grippers, grasping and control strategies, as well as their applications in agricultural robots: A review. *Comput. Electron. Agric.* **2020**, *177*, 105694. [CrossRef]
2. Takacs, K.; Mason, A.; Christensen, L.B.; Haidegger, T. Robotic grippers for large and soft object manipulation. In Proceedings of the 20th IEEE International Symposium on Computational Intelligence and Informatics, CINTI 2020—Proceedings, Budapest, Hungary, 5–7 November 2020. [CrossRef]
3. Zhakypov, Z.; Heremans, F.; Billard, A.; Paik, J. An origami-inspired reconfigurable suction gripper for picking objects with variable shape and size. *IEEE Robot. Autom. Lett.* **2018**, *3*, 2894–2901. [CrossRef]
4. Mahmoud, K.H.; Abdel-Jaber, G.T.; Sharkawy, A.N. Neural Network-Based Classifier for Collision Classification and Identification for a 3-DOF Industrial Robot. *Automation* **2024**, *5*, 13–34. [CrossRef]
5. Sharkawy, A.N. Task Location to Improve Human–Robot Cooperation: A Condition Number-Based Approach. *Automation* **2023**, *4*, 263–290. [CrossRef]
6. Jadhav, R.; Kamble, Y.G. Designing and Optimization of Mechanical Gripper Finger Using Finite Element Analysis. In *Techno-Societal 2022*; Springer: Cham, Switzerland, 2024. [CrossRef]
7. Malik, R.; Verma, Y.; Verma, A.; Rastogi, V. Grasping Force Analysis of 3-Fingered Gripper. In *Lecture Notes in Mechanical Engineering*; Springer: Singapore, 2022. [CrossRef]
8. Gabriel, F.; Fahning, M.; Meiners, J.; Dietrich, F.; Dröder, K. Modeling of vacuum grippers for the design of energy efficient vacuum-based handling processes. *Prod. Eng.* **2020**, *14*, 545–554. [CrossRef]
9. Maggi, M.; Mantriota, G.; Reina, G. Introducing POLYPUS: A novel adaptive vacuum gripper. *Mech. Mach. Theory* **2022**, *167*, 104483. [CrossRef]
10. Zhu, H.; Lin, Z.; Yan, J.; Ye, P.; Zhang, W.; Mao, S.; Guan, Y. Compact lightweight magnetic gripper designed for biped climbing robots based on coaxial rotation of multiple magnets. *Robot. Auton. Syst.* **2022**, *155*, 104164. [CrossRef]
11. Son, C.H.; Jeong, S.; Lee, S.; Ferreira, P.M.; Kim, S. Tunable Adhesion of Shape Memory Polymer Dry Adhesive Soft Robotic Gripper via Stiffness Control. *Robotics* **2023**, *12*, 59. [CrossRef]
12. Kostov, B.; Hristov, V. Comparision Between the Performance of Pneumatical and Electrical Grippers for Industrial Robots. In Proceedings of the 2023 11th International Scientific Conference on Computer Science, COMSCI 2023—Proceedings, Sozopol, Bulgaria, 18–20 September 2023. [CrossRef]
13. Long, Z.; Jiang, Q.; Shuai, T.; Wen, F.; Liang, C. A Systematic Review and Meta-analysis of Robotic Gripper. In *IOP Conference Series: Materials Science and Engineering*; IOP Publishing Ltd.: Bristol, UK, 2020. [CrossRef]

14. Diveev, A.; Shmalko, E.; Serebrenny, V.; Zentay, P. Fundamentals of synthesized optimal control. *Mathematics* **2021**, *9*, 21. [CrossRef]
15. Soliman, A.M.; Zaki, A.M.; El-Shafei, A.M.; Mahgoub, O.A. A robotic gripper based on advanced system set-up and fuzzy control algorithm. In Proceedings of the 2009 IEEE International Conference on Automation and Logistics, ICAL 2009, Shenyang, China, 5–7 August 2009. [CrossRef]
16. Vaishnav, S.; Khan, Z. Design and performance of PID and fuzzy logic controller with smaller rule set for higher order system. In Proceedings of the World Congress on Engineering and Computer Science 2007 WCECS 2007, San Francisco, CA, USA, 24–26 October 2007.
17. Tamilselvan, G.M.; Aarthy, P. Online tuning of fuzzy logic controller using Kalman algorithm for conical tank system. *J. Appl. Res. Technol.* **2017**, *15*, 492–503. [CrossRef]
18. Bachi, I.O.; Bahedh, A.S.; Kheioon, I.A. Design of control system for steel strip-rolling mill using NARMA-L2. *J. Mech. Sci. Technol.* **2021**, *35*, 1429–1436. [CrossRef]
19. Caccia, M.; Bibuli, M.; Bono, R.; Bruzzone, G. Basic navigation, guidance and control of an Unmanned Surface Vehicle. *Auton. Robot.* **2008**, *25*, 349–365. [CrossRef]
20. Yager, R.R.; Zadeh, L.A. (Eds.) *An Introduction to Fuzzy Logic Applications in Intelligent Systems*; Springer: New York, NY, USA, 1992. [CrossRef]
21. Somwanshi, D.; Bundele, M.; Kumar, G.; Parashar, G. Comparison of fuzzy-PID and PID controller for speed control of DC motor using LabVIEW. *Procedia Comput. Sci.* **2019**, *152*, 252–260. [CrossRef]
22. Aslinezhad, M.; Malekijavan, A.; Abbasi, P. Adaptive neuro-fuzzy modeling of a soft finger-like actuator for cyber-physical industrial systems. *J. Supercomput.* **2021**, *77*, 2624–2644. [CrossRef]
23. Nguyen, T.V.T.; Huynh, N.T.; Vu, N.C.; Kieu, V.N.D.; Huang, S.C. Optimizing compliant gripper mechanism design by employing an effective bi-algorithm: Fuzzy logic and ANFIS. *Microsyst. Technol.* **2021**, *27*, 3389–3412. [CrossRef]
24. Dinh, V.B.; Tran, N.T.; Dao, T.P. An integration framework of topology method, enhanced adaptive neuro-fuzzy inference system, water cycle algorithm with evaporation rate for design optimization for a flexure gripper. *Neural Comput. Appl.* **2022**, *34*, 349–374. [CrossRef]
25. Huynh, B.P.; Kuo, Y.L. Optimal fuzzy impedance control for a robot gripper using gradient descent iterative learning control in fuzzy rule base design. *Appl. Sci.* **2020**, *10*, 3821. [CrossRef]
26. Mukhtar, M.; Khudher, D.; Kalganova, T. A control structure for ambidextrous robot arm based on Multiple Adaptive Neuro-Fuzzy Inference System. *IET Control. Theory Appl.* **2021**, *15*, 1518–1532. [CrossRef]
27. Bahedh, A.S.; Kheioon, I.A.; Munahi, B.S.; Al-Sabur, R. Modelling and controlling of modified robotic gripper mechanism using intelligent technique scheme. In Proceedings of the 2022 Iraqi International Conference on Communication and Information Technologies, IICCIT 2022, Basrah, Iraq, 7–8 September 2022. [CrossRef]
28. Hazem, B.; Bingül. A comparative study of anti-swing radial basis neural-fuzzy LQR controller for multi-degree-of-freedom rotary pendulum systems. *Neural Comput. Appl.* **2023**, *35*, 17397–17413. [CrossRef]
29. de Campos Souza, P.V. Fuzzy neural networks and neuro-fuzzy networks: A review the main techniques and applications used in the literature. *Appl. Soft Comput. J.* **2020**, *92*, 106275. [CrossRef]
30. Vashishtha, S.; Gupta, V.; Mittal, M. Sentiment analysis using fuzzy logic: A comprehensive literature review. *WIREs Data Min. Knowl. Discov.* **2023**, *13*, e1509. [CrossRef]
31. Sadighi, M.; Motamedvaziri, B.; Ahmadi, H.; Moeini, A. Assessing landslide susceptibility using machine learning models: A comparison between ANN, ANFIS, and ANFIS-ICA. *Environ. Earth Sci.* **2020**, *79*, 536. [CrossRef]
32. Wang, G.; Zhou, T.; Choi, K.S.; Lu, J. A Deep-Ensemble-Level-Based Interpretable Takagi-Sugeno-Kang Fuzzy Classifier for Imbalanced Data. *IEEE Trans. Cybern.* **2022**, *52*, 3805–3818. [CrossRef] [PubMed]
33. Pal, D.; Bhagat, S.K. Design and Analysis of Optimization based Integrated ANFIS- PID Controller for Networked Controlled Systems (NCSs). *Cogent Eng.* **2020**, *7*, 1772944. [CrossRef]
34. Najib, M.; Salleh, M.; Talpur, N.; Hussain, K. Adaptive Neuro-Fuzzy Inference System: Overview, Strengths, Limitations, and Solutions. In *Lecture Notes in Computer Science*; LNISA; Springer: Cham, Switzerland, 2017; Volume 10387, pp. 527–535. [CrossRef]
35. Khuntia, S.R.; Panda, S. ANFIS approach for SSSC controller design for the improvement of transient stability performance. *Math. Comput. Model.* **2013**, *57*, 289–300. [CrossRef]
36. Vargas, O.S.; De Leon Aldaco, S.E.; Alquicira, J.A.; Vela-Valdes, L.G.; Nunez, A.R.L. Adaptive Network-Based Fuzzy Inference System (ANFIS) Applied to Inverters: A Survey. *IEEE Trans. Power Electron.* **2024**, *39*, 869–884. [CrossRef]
37. Datta, R.; Saravanakumar, R.; Dey, R.; Bhattacharya, B.; Ahn, C.K. Improved stabilization criteria for Takagi–Sugeno fuzzy systems with variable delays. *Inf. Sci.* **2021**, *579*, 591–606. [CrossRef]
38. Elouni, M.; Hamdi, H.; Rabaoui, B.; Braiek, N.B. Adaptive PID Fault-Tolerant Tracking Controller for Takagi-Sugeno Fuzzy Systems with Actuator Faults: Application to Single-Link Flexible Joint Robot. *Int. J. Robot. Control. Syst.* **2022**, *2*, 523–546. [CrossRef]

39. Ghany, M.A.A.; Bahgat, M.E.; Refaey, W.M.; Sharaf, S. Type-2 fuzzy self-tuning of modified fractional-order PID based on Takagi–Sugeno method. *J. Electr. Syst. Inf. Technol.* **2020**, *7*, 2. [CrossRef]
40. Alavala, C.R. *Fuzzy Logic and Neural Networks: Basic Concepts & Application*; New Age International Publishers: New Delhi, India, 2017.
41. Koustoumpardis, P.N.; Smyrnis, S.; Aspragathos, N.A. A 3-finger robotic gripper for grasping fabrics based on cams-followers mechanism. In *Mechanisms and Machine Science*; Springer: Cham, Switzerland, 2018; Volume 49, pp. 612–620. [CrossRef]
42. Silva-Caballero, A.; González-Palacios, M.A.; Aguilera-Cortés, L.A. Implementation of the Slide-O-Cam mechanism in the design of a robot gripper. In Proceedings of the 13th World Congress in Mechanism and Machine Science, Guanajuato, Mexico, 19–23 June 2011; pp. 19–25.
43. Dang, T.N. Design and Simulation of a New Concentric Gripper with Two-Finger and Support Bar Driven by a Wedge Cam. In *Lecture Notes in Networks and Systems*; LNNS; Springer Nature: Cham, Switzerland, 2024; Volume 943, pp. 352–366. [CrossRef]
44. Pozzi, M.; Achilli, G.M.; Valigi, M.C.; Malvezzi, M. Modeling and Simulation of Robotic Grasping in Simulink Through Simscape Multibody. *Front. Robot. AI* **2022**, *9*, 873558. [CrossRef] [PubMed]
45. Hassan, A.; Abomoharam, M. Modeling and design optimization of a robot gripper mechanism. *Robot. Comput.-Integr. Manuf.* **2017**, *46*, 94–103. [CrossRef]
46. Ferretti, G.; Magnani, G.; Rocco, P.; Viganò, L. Modelling and simulation of a gripper with Dymola. *Math. Comput. Model. Dyn. Syst.* **2006**, *12*, 89–102. [CrossRef]
47. Rawashdeh, N.; Abu-Alrub, N. Gripper control design and simulation for openrov submarine robot. *Actuators* **2021**, *10*, 252. [CrossRef]
48. Datta, R.; Pradhan, S.; Bhattacharya, B. Analysis and Design Optimization of a Robotic Gripper Using Multiobjective Genetic Algorithm. *IEEE Trans. Syst. Man Cybern. Syst.* **2016**, *46*, 16–26. [CrossRef]
49. Aslam, M.S.; Tiwari, P.; Pandey, H.M.; Band, S.S.; El Sayed, H. A delayed Takagi–Sugeno fuzzy control approach with uncertain measurements using an extended sliding mode observer. *Inf. Sci.* **2023**, *643*, 119204. [CrossRef]
50. Aslam, M.S.; Tiwari, P.; Pandey, H.M.; Band, S.S. Robust stability analysis for class of Takagi-Sugeno (TS) fuzzy with stochastic process for sustainable hypersonic vehicles. *Inf. Sci.* **2023**, *641*, 119044. [CrossRef]
51. Aslam, M.S.; Bilal, H.; Band, S.S.; Ghasemi, P. Modeling of nonlinear supply chain management with lead-times based on Takagi-Sugeno fuzzy control model. *Eng. Appl. Artif. Intell.* **2024**, *133*, 108131. [CrossRef]
52. Tran, N.T.; Dang, M.P.; Dao, T.P. A new optimal design synthesis method for flexure-based mechanism: Recent advance of metaheuristic-based artificial intelligence for precision micropositioning system. *Microsyst. Technol.* **2024**, *30*, 1–31. [CrossRef]
53. Karsaz, A. Chattering-free hybrid adaptive neuro-fuzzy inference system-particle swarm optimisation data fusion-based BG-level control. *IET Syst. Biol.* **2020**, *14*, 31–38. [CrossRef]
54. Hussain, W.; Merigó, J.M.; Raza, M.R.; Gao, H. A new QoS prediction model using hybrid IOWA-ANFIS with fuzzy C-means, subtractive clustering and grid partitioning. *Inf. Sci.* **2022**, *584*, 280–300. [CrossRef]
55. Abdullahi, S.B.; Muangchoo, K.; Abubakar, A.B.; Ibrahim, A.H.; Aremu, K.O. Data-Driven AI-Based Parameters Tuning Using Grid Partition Algorithm for Predicting Climatic Effect on Epidemic Diseases. *IEEE Access* **2021**, *9*, 55388–55412. [CrossRef]
56. Zanganeh, M. Improvement of the ANFIS-based wave predictor models by the Particle Swarm Optimization. *J. Ocean. Eng. Sci.* **2020**, *5*, 84–99. [CrossRef]
57. Ghobadiha, Y.; Motieyan, H. Urban growth modelling in Qazvin, Iran: An investigation into the performance of three ANFIS methods. *J. Spat. Sci.* **2023**, *68*, 523–542. [CrossRef]
58. Ramadan, A.; Kamel, S.; Hamdan, I.; Agwa, A.M. A Novel Intelligent ANFIS for the Dynamic Model of Photovoltaic Systems. *Mathematics* **2022**, *10*, 1286. [CrossRef]
59. Al-Gathe, A.A.; Baarimah, S.O.; Al-Khudafi, A.M. Modelling gas compressibility factor using different fuzzy methods. *AIP Conf. Proc.* **2022**, *2443*, 030031. [CrossRef]
60. Bobyr, M.V.; Emelyanov, S.G. A nonlinear method of learning neuro-fuzzy models for dynamic control systems. *Appl. Soft Comput. J.* **2020**, *88*, 106030. [CrossRef]
61. Jawad, Q.A.; Mohammed, R.J.; Hadi, A.K.; Kheioon, I.A. Liquid Level Controlling Using the Intelligent Techniques. In Proceedings of the 2023 7th International Symposium on Multidisciplinary Studies and Innovative Technologies (ISMSIT), Ankara, Turkiye, 26–28 October 2023. [CrossRef]
62. Rojas-García, L.N.; Chávez-Olivares, C.A.; Bonilla-Gutiérrez, I.; Mendoza-Gutiérrez, M.O.; Ramírez-Cardona, F. Force/position control with bounded actions on a dexterous robotic hand with two-degree-of-freedom fingers. *Biocybern. Biomed. Eng.* **2022**, *42*, 233–246. [CrossRef]
63. Cortinovis, S.; Vitrani, G.; Maggiali, M.; Romeo, R.A. Control Methodologies for Robotic Grippers: A Review. *Actuators* **2023**, *12*, 332. [CrossRef]

64. Sadun, A.S.; Jalani, J.; Sukor, J.A.; Jamil, F. Force control for a 3-Finger Adaptive Robot Gripper by using PID controller. In Proceedings of the 2016 2nd IEEE International Symposium on Robotics and Manufacturing Automation (ROMA), Ipoh, Malaysia, 25–27 September 2016; pp. 1–6. [CrossRef]
65. Vitrani, G.; Cortinovis, S.; Fiorio, L.; Maggiali, M.; Romeo, R.A. Improving the Grasping Force Behavior of a Robotic Gripper: Model, Simulations, and Experiments. *Robotics* **2023**, *12*, 148. [CrossRef]